FLOW CHARACTERIZATION STUDY AND FIRE EXPERIMENTS IN A REDUCED SCALED TUNNEL

A THESIS SUBMITTED TO
THE GRADUATE SCHOOL OF NATURAL AND APPLIED SCIENCES
OF
MIDDLE EAST TECHNICAL UNIVERSITY

BY

MAJD BASIL ABDEL MUHSEN ABUAISHEH

IN PARTIAL FULFILLMENT OF THE REQUIREMENTS
FOR
THE DEGREE OF MASTER OF SCIENCE
IN
MECHANICAL ENGINEERING

JANUARY 2019

Approval of the thesis:

FLOW CHARACTERIZATION STUDY AND FIRE EXPERIMENTS IN A REDUCED SCALED TUNNEL

submitted by **MAJD BASIL ABDEL MUHSEN ABUAISHEH** in partial fulfillment of the requirements for the degree of **Master of Science in Mechanical Engineering Department, Middle East Technical University** by,

Prof. Dr. Halil Kalıpçılar
Dean, Graduate School of **Natural and Applied Sciences** ____________________

Prof. Dr. M. A. Sahir Arıkan
Head of Department, **Mechanical Engineering** ____________________

Assoc. Prof. Dr. Ahmet Yozgatlıgil
Supervisor, **Mechanical Engineering, METU** ____________________

Assoc. Prof. Dr. M. Metin Yavuz
Co-Supervisor, **Mechanical Engineering, METU** ____________________

Examining Committee Members:

Prof. Dr. M. Haluk Aksel
Mechanical Engineering, METU ____________________

Assoc. Prof. Dr. Ahmet Yozgatlıgil
Mechanical Engineering, METU ____________________

Assoc. Prof. Dr. M. Metin Yavuz
Mechanical Engineering, METU ____________________

Assist. Prof. Dr. Özgür Uğraş Baran
Mechanical Engineering, METU ____________________

Prof. Dr. Selin Aradağ Çelebioğlu
Mechanical Engineering, TOBB ETÜ ____________________

Date: 30.01.2019

I hereby declare that all information in this document has been obtained and presented in accordance with academic rules and ethical conduct. I also declare that, as required by these rules and conduct, I have fully cited and referenced all material and results that are not original to this work.

Name, Surname: Majd Basil Abdel Muhsen Abuaisheh

Signature:

ABSTRACT

FLOW CHARACTERIZATION STUDY AND FIRE EXPERIMENTS IN A REDUCED SCALED TUNNEL

Abuaisheh, Majd Basil Abdel Muhsen
Master of Science, Mechanical Engineering
Supervisor: Assoc. Prof. Dr. Ahmet Yozgatlıgil
Co-Supervisor: Assoc. Prof. Dr. M. Metin Yavuz

January 2019, 83 pages

This work is an experimental study on the subject of tunnel fires, which is conducted on a ventilated 1/13 scaled tunnel model in the Fluid Mechanics Laboratory, Department of Mechanical Engineering of Middle East Technical University. In order to perform the experiments, in the first stage, the tunnel model was completely renovated, and its overall condition was improved to obtain better means of control and accuracy on the experimental measurements. In the second stage of the thesis, a flow characterization study was conducted on the flow inside the tunnel model under fire (hot flow) and cold flow conditions using Laser Doppler Anemometry (LDA) optical method to identify the ventilation velocity profile, improve its uniformity and understand the mutual effects between fire and the ventilation flow in the upstream of fire. For the hot flow cases, ethanol pools were used as the fire source. The effect of tunnel ventilation velocity on important fire parameters such as flow temperature and heat release rate of fire were investigated. Results showed that the critical ventilation velocity of the tunnel is achieved around 0.85 m/s. The flow inside the model tunnel is highly affected by the fire in the downstream due to buoyancy effect of the smoke that resists the bulk motion of the airflow. It was shown that heat release rate and gas temperature of the tunnel are functions of ventilation velocity as well.

Keywords: Scaled Tunnel Model, Pool Fire, Heat Release Rate, Flow Characterization, Ventilation Velocity

ÖZ

ÖLÇEKLİ TÜNEL MODELİNDE BİR AKIŞ KARAKTERİZASYONU ÇALIŞMASI VE YANGIN DENEYLERİ

Abuaisheh, Majd Basil Abdel Muhsen
Yüksek Lisans, Makina Mühendisliği
Tez Danışmanı: Doç. Dr. Ahmet Yozgatlıgil
Ortak Tez Danışmanı: Doç. Dr. M. Metin Yavuz

Ocak 2019, 83 sayfa

Bu çalışma, Orta Doğu Teknik Üniversitesi, Makina Mühendisliği Bölümü, Akışkanlar Mekaniği Laboratuvarında bulunan havalandırmalı 1/13 ölçekli tünel modeli kullanılarak tünel yangınları üzerinde deneysel olarak yapılmıştır. Deneylerin gerçekleştirilmesi için, ilk aşamada, tünel modelinin yapısı yenilenmiş ve daha kontrollü ölçümlerin eldesi için modelin genel durumu iyileştirilmiştir. Çalışmanın ikinci aşamasında, Lazer Doppler Anemometrisi (LDA) optik metodu kullanılarak tünel modelinin içindeki yangın (sıcak akış) ve soğuk akış koşulları altında akış karakterizasyonu çalışması yapılmıştır. Bu çalışma neticesinde havalandırma hızının profili belirtilmiş, üniformluğu iyileştitilmiş, ve yangın ile havalandırma akışının arasındaki etkileşim incelenmiştir. Çalışmada yangın kaynağı olarak etanol havuzları kullanılmıştır. Tünel havalandırma hızının, sıcaklık dağılımı ve yangının ısı salınım hızı gibi önemli yangın parametreleri üzerindeki etkisi araştırılmıştır. Sonuçlar, tünelin kritik havalandırma hızının yaklaşık olarak 0,85 m/s olduğunu göstermiştir. Sonuçlar ayrıca tüneldeki akışın yangından kaynaklanan dumanın kaldırma kuvveti ve akış kütlesine karşı oluşan dirençten dolayı oldukça etkilendiğini göstermektedir. Tünelin ısı salınım hızı ve sıcaklık dağılımı ise havalandırma hızına göre değiştiği gözlemlenmiştir.

Anahtar Kelimeler: Ölçekli Tünel Modeli, Havuz Yangını, Isı Salınım Hızı, Akış Karakterizasyonu, Havalandırma Hızı.

To my sister, Tasneem

ACKNOWLEDGMENTS

Foremost, I would like to express my gratitude to my supervisor, Professor Ahmet Yozgatlıgil for his continuous support and trusts throughout my studies. His patience, motivation and immense knowledge inspired me to purse my graduate studies since I first met him in my fourth year of my undergraduate study. He was always there for me with his guidance and recommendations. It was an honor having him an advisor and mentor for master's study.

Besides my advisor, I would like to thank my co-supervisor Professor Metin Yavuz for his encouragement and insightful guidance. His door was open to me whenever I ran into a trouble spot or had a question about my research. Without his guidance and suggestions, this research could not have been successfully conducted.

My sincere thanks also go to Mr. Mehmet Özçiftçi, Ms. Burcu Karagöz and Mr. Kayacan Kestel from the Fluid Mechanics Laboratory of METU for their technical assistance with the experimental setup. I would also like to thank my fellows in the Internal Combustion Laboratory; Mr. Levent Şahin, Mr. Ramin Barzegar and foremost, Dr. Sina Soylu who shared his immense knowledge and experience with me and help me overcoming all the challenges and hard times during my study, I can't find words to express my gratitude to him.

Finally, I must express my very profound gratitude to my family for providing me with unfailing support and continuous encouragement throughout my years of study. My parents, Basil and Naheel, my brothers Ahmad and Haytham, my beloved sisters Tasneem, Haneen and Sireen; you are the everything to me, without you I would not be where I am today. I love you all.

TABLE OF CONTENTS

LIST OF TABLES

LIST OF FIGURES

LIST OF ABBREVIATIONS

FDS	Fire Dynamics Simulator
Fr	Froude number
HGV	Heavy Good Vehicle
NFPA	National Fire Protection Association
CH	Channel number in the data logger
HRR	Heat Release Rate
LDA	Laser Doppler Anemometry
MLR	Mass Loss Rate

LIST OF SYMBOLS

A	: Pool surface area	[m²]
A	: Cross sectional area of the tunnel	[m²]
c_p	: Specific heat	[W/m^{2}K]
E	: Energy release	[J]
g	: Gravitational acceleration	[m/s²]
H_c	: Heat of combustion	[J]
H	: Tunnel height	[m]
k	: Thermal conductivity	[W/mK]
m	: Mass	[kg]
m	: Mass flow rate	[kg/s]
m'	: Burning rate	[kg/m^{2}s]
Q	: Heat release rate	[W]
ρ	: Density	[kg/m^3]
T	: Temperature	[°C], [K]
t	: Time	[s]
u,V	: Velocity	[m/s]
V^*	: Non-dimensional velocity	
x	: Position	[m]

Subscripts

A	: Air
c	: Convective, Combustion
$cond$	: Conduction
$conv$	: Convection
cr	: Critical
F	: Full scale

g : Gasification, gaseous state

i : Initial state

Superscripts

A : Analyzer

* : Dimensionless analysis symbol

+ : Non-dimensionalization symbol

o : Standard condition symbol

CHAPTER 1

INTRODUCTION

Throughout history, the mankind has developed various ways to transfer goods and passengers. Until 3500 BC, animals were the only way of transportation, then a breakthrough took place when the wheel was invented, and later, the invention of the first sailing boat [1]. Yet, the most dramatic development in transportation was during the industrial revolution in the 17th and 18th century when many new modes of transportation were invented such as cars, trains, trucks and airplanes [2]. However, the new challenge was to overcome the alleviating traffic congestion and the rough terrains that became serious problems as the human societies started to expand. But the most efficient, and the most used means are tunnels. As more tunnels are constructed day by day, and as traffic is getting heavier, more fire incidents threaten the lives of the passengers. Due to the confined structure of tunnels, if a fire accident occurs, the temperature increases rapidly which risks the lives of the passengers together with the risk of suffocation due to oxygen depletion and toxic gas inhalation. Many catastrophic incidents have happened since the last century like the incidents of Mont Blanc, Tauern, and St. Gotthard which resulted in the death of tens of people. Those incidents drew the attention to the importance of studying fires in tunnels.

The fire safety systems in tunnels are designed to control the fire in a way that allows the rescue teams to evacuate the passengers in any fire scenario that might occur. These systems are concerned with control of the increasing temperature due to fire so that it does not exceed the limits that threatens the passengers. These safety factors are also concerned with smoke control by supplying ventilating air to control smoke movement in the tunnel and providing fresh air to save passengers from suffocation.

Over the years, researchers have studied fires in tunnels to provide the necessary data to design more sophisticated fire safety systems. Many experimental and numerical studies try to understand how fire evolves and how it is affected by various factors related to ventilation, tunnel geometry, etc. As more studies are carried out on tunnel fires, the state of knowledge related to the topic will be more enriched, which results in better and more reliable fire safety systems and that what is the motivation for conducting this research work.

1.1. Confinement fires

Fires in confined space exhibit five stages as shown in Figure 1.1. Ignition starts when sufficient amount of energy, e.g. a spark, is supplied to the burning fuel in the presence of oxygen. If the oxygen supply is sufficient, fire passes to fire growth stage and it is referred as "fuel controlled". An abrupt increase in Heat Release Rate (HRR) takes place when the radiation from the hot gases starts to dominate resulting in ignition of unburnt fuel, this stage is referred as the flash over stage. As the supplied air cannot catch up with the increase in HRR, the HRR reaches a peak value in the fully developed fire stage. This stage is often called oxygen (ventilation) controlled stage due to lower oxygen availability. The last stage is decay, as the fuel runs out.

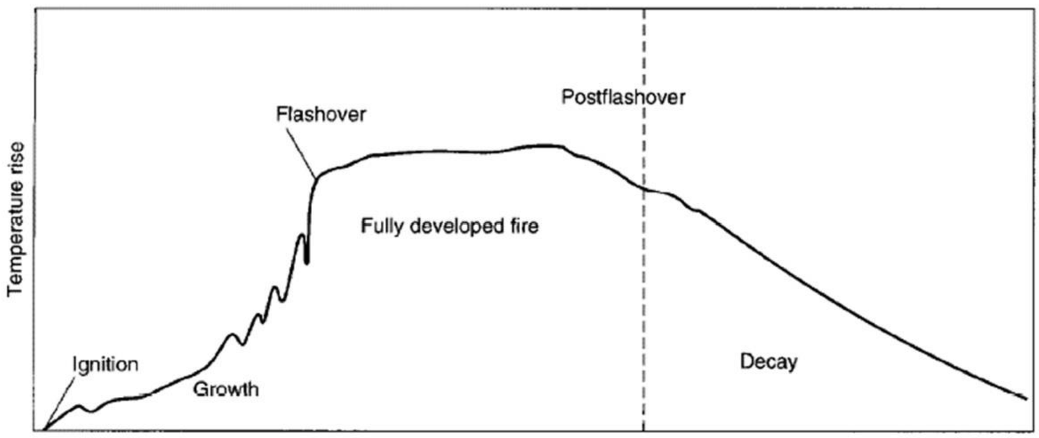

Figure 1.1. Evolution of compartment fire [3]

1.2. Aims of the thesis

The aim of this study was to renovate a current experimental setup to perform more controlled fire experiments in tunnels. Effect of tunnel fire on the incoming ventilation flow to the tunnel was investigated and different fire characteristics such as temperature, heat release rate and burning rate were studied. Therefore, the work can be categorized in three main sections as below:

1.2.1. Renovating the tunnel model

The previous tunnel model, which was used in studying realistic fire scenarios was renovated by renewing the main parts of the model tunnel and addition of new and more controllable equipment.

1.2.2. Flow characterization of the tunnel ventilation

Even though fire characteristics are affected by velocity profile of the ventilating air, there is no major report in the literature that studies the effect of fire on upstream flow conditions. Studying the effect of fire in the upstream section of the tunnel is important because fire safety devices take into account the temperature and ventilation conditions of the upstream of fire as well. Therefore, flow characterization of the ventilating air was conducted using Laser Doppler Anemometry (LDA) method both in the hot flow, where combustion is taking place in the tunnel, and in the clod flow, where there is no fire in the model. This will give an idea about the effect of the fire on the velocity profile of the ventilating air.

1.2.3. Study on the effect of ventilation on fire temperature and heat release rate

Temperature distribution along the ceiling of the tunnel is important in designing fire-proofing materials and lining structures in tunnels [4]. Studying the effect of ventilation on temperature distribution gives an idea about the critical ventilation velocity, which is the minimum steady state velocity of the ventilation airflow moving toward the fire, within a tunnel or passageway, that is required to prevent backlayering at the fire site [5]. In the literature, there are proposed models to predict the critical ventilation velocity depending on different factors such as HRR and tunnel cross-section. In this work, the effect of tunnel ventilation on HRR of fire and temperature distribution will be studied with a more controlled means for ventilation, and the critical ventilation velocity will be compared with proposed models in the literature and previous works conducted using this setup.

1.3. Thesis outline

This thesis is organized as follows. Chapter II gives brief information about the history of fires in tunnels and the safety factors and standards used in the literature. In Chapter III, the renovation steps of the previous setup are discussed. Chapter IV discusses the experimental equipment and the methods used in this study. Results for flow characterization and pool fire experiments are presented in Chapter V and finally, conclusive remarks are made in Chapter VI.

CHAPTER 2

LITERATURE SURVEY

While statistics show far lower rate of accidents inside tunnels compared to accidents in open roads [6], still accidents inside tunnels are more catastrophic due to the enclosed structure of tunnels, which makes it difficult to suppress and extinguish the fire. In addition to heat load, smoke and toxic gas suffocation are serious threatens to the lives of the motorists inside tunnels. In 1921, two trains collided inside Batignolles tunnel in Paris, the collision caused the death of some people, but even more people died because of the fire caused by discharging gases from the illumination system which caught fire [7]. This accident left 28 fatalities and drew attention to the importance of having fire safety systems as it was the first fire incident in a tunnel. In 1944, in Armi Tunnel in Balvano in Italy, a train got stuck in highly inclined tunnel, until the train had gone back out of the tunnel, 426 people died due to suffocation of carbon monoxide that is emitted from the coal burning. Table 2.1 lists many incidents that took place since 1921 in tunnels, the high numbers of casualties show the importance of studying fires in tunnels and developing best fire safety systems to avoid regrettable consequences.

Table 2.1. *List of tunnel incidents since 1921 [6, 8, 7, 9]*

Year	Tunnel Name	Country	Cause	Casualties
1921	Batignolles	France	Front-rear train collision	more than 28 dead
1944	Armi Tunnel	Italy	Carbon monoxide poisoning	426 dead 60 injured
1971	Vranduk	Yugoslavia	Diesel-electrical engine caught Fire	34 dead 113 injured
1972	Hokuriku	Japan	A dining car caught fire	30 dead many injured
1979	Nihonzaka	Japan	Collision of vehicles	7 dead 1 injured
1982	Caldecott	USA	Collision and fuel leakage	7 dead 2 injured
1982	Salang	Afghanistan	Collision	> 400 dead
1983	Pecorila Galleria	Italy	-	9 dead 22 injured
1987	King’s Cross Metro station	UK	Fire in escalator	31 dead many injured
1995	Baku Metro	Azerbaijan	Fire due to electrical fault	289 dead 265 injured
1999	Mont Blanc	France/Italy	Oil leakage	39 dead 27 injured
1999	Tauern	Austria	Collision	12 dead 49 injured
2000	Kitzsteinhorn	Austria	A cable car caught fire	155 dead
2001	St. Gotthard	Switzerland	Collision between 2 HGVs	11 dead
2003	Daegu	South Korea	An arsonist set fire to a train	192 dead 151 injured
2006	Viamala	Switzerland	Collision	9 dead 6 injured

2.1. Standards used in designing tunnel fire safety

As the catastrophic incidents drew more attention to the importance of having well designed fire safety systems, the Permanent International Association of Road Congresses (PIARC) Committee on Road Tunnels was created in 1957. The committee was firstly concerned with safety equipment related to fires, then it became concerned with ventilation for smoke control. This committee was presenting data and recommendations in reports for the World Road Congress. Later in 1992, the Committee on Road Tunnels decided to create a group devoted for Fire and Smoke Control. This group presented its first report in 1995 after the committee worked on several research programs. The report provides the complete state of art prepared by the working group. It gives people who work on tunnel design and construction some background together with an overview and recommendations on the way to design efficient and cost-effective protection systems against fire and smoke. The report discusses the researches done on topics related to fire safety in tunnels including ventilation, exits and other safety facilities, fire response management, tunnel reaction and resistance to fire and smoke behavior, and it provides general guidelines and recommendations for the designers [9].

Another widely used standard in tunnel fires is the one provided by the National Fire Protection Association (NFPA) of the code 502. The Technical Committee on Motor Vehicle Fire Protection prepared NFPA 502 “Standard for Limited Access Highways, Tunnels, Bridges, and Elevated Structures” and it was adopted by the NFPA in 1972. The document has gone through many revisions and updates since then, and many new chapters were added until it reached its final version in the 2017 edition. The additions and updates are mainly based on full-scale test programs held by the Technical Committee on Motor Vehicle Fire Protection together with the work available in the literature. NFPA 502 provides more advanced and more detailed guidelines compared to the report published by PIARC which makes it the most used standard for designing fire safety systems. NFPA 502 gives general background and definitions for the designers, then it refers to the previous work and research done on tunnel fires later it mentions requirements such as emergency response plan, emergency communications, structural anchorage, etc. The standard illustrates the requirements for the safety system like fans and sprinklers, it explains how to choose the appropriate size and place. The standard also gives guidelines for emergency ventilation, it explains how it can be used in smoke control and how it is related to heat load, all the guidelines are supported with mathematical description. The standard also discusses the design of water supply systems, electrical systems and control systems [5]. In addition to NFPA 502 and PIARC, ASHRAE included a section about tunnel fires in its handbook for HVAC applications [6].

2.2 Types of ventilation systems in tunnels

Ventilation is necessary in most of tunnels as it controls the concentrations of contaminants and keep it at acceptable levels, and it is important to control the smoke in case of a fire in the tunnel. Some tunnels are ventilated naturally, while others, especially those of length more than 1000 m, need a mechanical or fan-driven ventilation system [5]. Those systems are classified into longitudinal or transverse ventilation systems. In longitudinal ventilation systems, fresh air is supplied through the entry portal and expelled out of the exit portal by means of jet fans. While in transverse systems, fresh air is supplied transversely across the tunnel by means of two ducts, one for the entering fresh air and the other for expelling the exhaust air as shown in Figure 2.1[10]. There are other ventilation systems including semi-transverse and partial transverse ventilation, those systems are discussed in the work of Chow et al. after conducting numerical simulation for each type to discuss its advantages and disadvantages as illustrated in Table 2.2 [11]. Most of the old tunnels have transverse ventilation systems whereas in recent years, longitudinal systems are more used in the eastern countries. In the USA, the most used type is the transverse while in Europe both transverse and longitudinal systems are used [12].

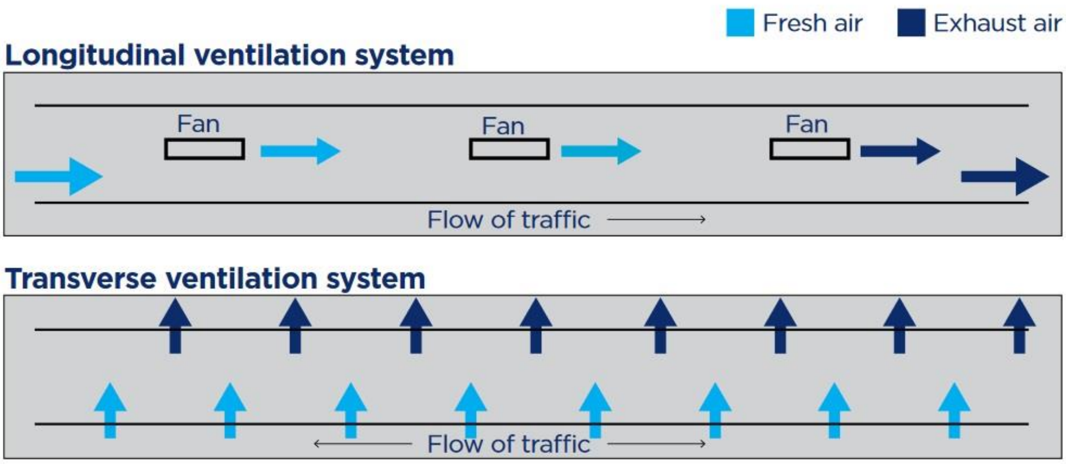

Figure 2.1. Longitudinal and transverse ventilation systems

Table 2.2. *Advantages and disadvantages of different ventilation systems [11]*

Ventilation system type	Advantages	Disadvantages
Longitudinal	Low cost, less space, simple installation, good smoke control	Limited to unidirectional traffic and high portal emission
Transverse	Applicable for bidirectional traffic, suitable for long tunnels, effective in temperature management	Ineffective in smoke management, high investment cost
Semi-transverse	Low maintenance cost, clear zones on both sides of fire, smoke is removed from tunnel	No directional smoke control, high investment cost
Combination of longitudinal and semi-transverse systems	Smaller critical velocity, clear zones on both sides, good smoke control,	High investment cost, complex system control

2.3 Scaling in fire research

In the standards and the literature of fire research, most of the data have been acquired based on large-scale tests. Large-scale fire tests are usually conducted in disused or in abandoned tunnels which makes it difficult and expensive for the fire researchers to conduct the tests. Therefore, in recent years, researchers have focused more on the reduced scaled models and related experiments to obtain a deeper understanding of tunnel fires. However, achieving complete similarity between large-scale and reduced-scale models is not possible due to inconsistencies in the nature of fire [13, 14]. Therefore, partial similarity is used in scaled tunnel fire studies, which is called Froude modelling technique. The Froude number is given in the following equation, where u is the ventilation velocity, g is the gravitational acceleration, and l is the length of the tunnel

$$Fr \approx \frac{u^2}{gl} = \frac{Inertial\ Forces}{Buoyancy\ Forces} \tag{2.7}$$

According to Froude modeling, relationships for the characteristic tunnel velocity, heat release rate and flow temperature can be established between model and the real scale tunnel as given in the following equations

$$\frac{\dot{Q}_M}{\dot{Q}_F} = (\frac{l_M}{l_F})^{5/2} \tag{2.8}$$

$$\frac{V_M}{V_F} = (\frac{l_M}{l_F})^{1/2} \tag{2.9}$$

$$T_M = T_F \tag{2.10}$$

where $\dot{Q}$ is the HRR, *T* is gas temperature in Kelvin, *V* is the characteristic velocity (in tunnel fires it is ventilation velocity), *M* stands for model and *F* stands for full scale. The scaling used in the model of this study is 1/13. Froude scaling is widely used is reduced-scale tunnel fire studies [15]. Using this scaling approach, Table 2.3 shows the equivalent HRR values in the real tunnel compared to model values.

Table 2.3. *Full-scale vs model HRR comparison [16]*

Model HRR (kw)	**Equivalent full scale HRR (MW)**	**Equivalent tunnel fire scenario**
3 – 14	1.5 – 8	Small cars
32 – 50	20 – 30	Truck or bus
21 – 328	13 – 202	Heavy good vehicle
12 – 70	7 – 43	Railroad Vehicle

2.4 Common terminology in fire research literature

In compartment fires, many factors need to be considered in designing fire safety systems. Fire engineers need to keep the highest possible control of those threatening factors such as heat load, temperature distribution, oxygen depletion and asphyxiation by inhaling smoke and fumes to provide effective means of escape and rescue. The safety measures mentioned in the fire safety standards such as NFPA 502 are certain requirements for the safety of the passengers inside the tunnel and the rescue teams and for the protection of the structural components of the tunnel.

2.4.1 Heat Release Rate of fire

HRR is considered as "*the single most important factor in fire hazard*" [17] [13, 18]. It represents the heat load of the fire and it relates to other factors as well such as temperature distribution and heat transfer. Also, HRR is used in characterizing the flammability of products and their consequent fire hazard which makes HRR the best predictor of fire hazard [17]. HRR can be measured using two methods, by measuring the mass loss rate (MLR) of the burning fuel and by using oxygen consumption calorimetry method (OCCM) when the MLR cannot be identified. [14, 19, 20, 21]. In the first method, the MLR is measured during the combustion process using a balance and then the MLR is multiplied by the heat of combustion to get the HRR. On the other hand, oxygen consumption calorimetry method is based on the oxygen depletion and variations in the concentration of combustion species. In this method, a gas analyzer is used to measure the concentration of the combustion products, those concentrations are plugged in the following equations

$$\dot{Q} = \left(\emptyset - \left(\frac{E'' - E'}{E'} \right) \left(\frac{1 - \emptyset}{2} \right) \frac{X_{CO}^{A}}{X_{O_2}^{A}} \right) X_{O_2}^{\circ} \dot{V}_A \tag{2.11}$$

$$\emptyset = \frac{X_{O_2}^{\circ} - X_{O_2}^{A} \left(1 - X_{CO_2}^{\circ} - X_{H_2O}^{\circ}\right) / \left(1 - X_{CO_2}^{A} - X_{CO}^{A}\right)}{X_{O_2}^{\circ} \left(1 - X_{O_2}^{A} / 1 - X_{CO_2}^{A} - X_{CO}^{A}\right)} \tag{2.12}$$

where X is the mole fraction of the species, the subscript '*o*' refers to standard conditions, while mole fractions with the subscript 'A' are the mole fractions measured by the gas analyzer, E' is the heat release of combustion per unit volume of oxygen consumed and equal to 17.2 MJ/m^3, E'' is the heat released per volume of oxygen consumed in the burning of CO and equal to 23.1 MJ/m^3 and $\emptyset$ is the oxygen depletion factor. Detailed derivations of equations (2.11) and (2.12) are explained in [17]. This method has been used extensively in literature [22, 23, 24, 25, 26] including tunnel fire research [27, 28, 29]

2.4.2 Critical ventilation velocity

It was stated that the most commonly used ventilation systems in designing fire safety systems in tunnels are the longitudinal ventilation systems [12]. In those systems, the fresh air is supplied longitudinally along the tunnel and it tries to push the smoke in the downstream direction, so an evacuation path is created for the passengers in the upstream direction. The critical ventilation velocity is defined as *"the minimum steady state velocity of the ventilation airflow moving toward the fire, within a tunnel or passageway, that is required to prevent backlayering at the fire site"* [5], while backlayering is defined as the movement of the smoke and hot gases counter to the direction of the ventilation airflow as shown in Figures 2.2 and 2.3 [5]. There are models that are proposed in the literature to predict the critical ventilation velocity in tunnels. Some of the common models are discussed in this section.

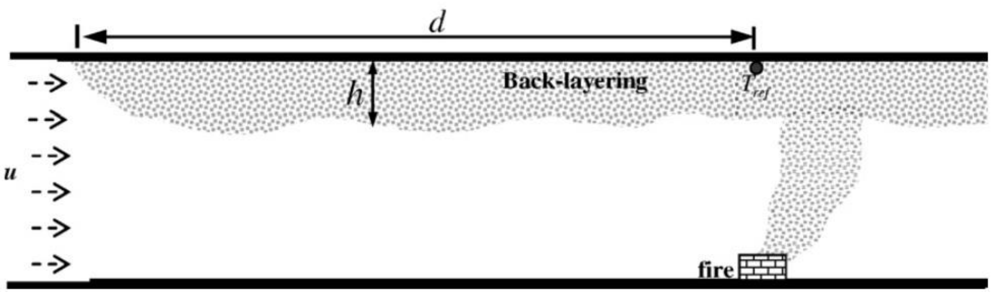

Figure 2.2. Back-layering length in tunnel fire

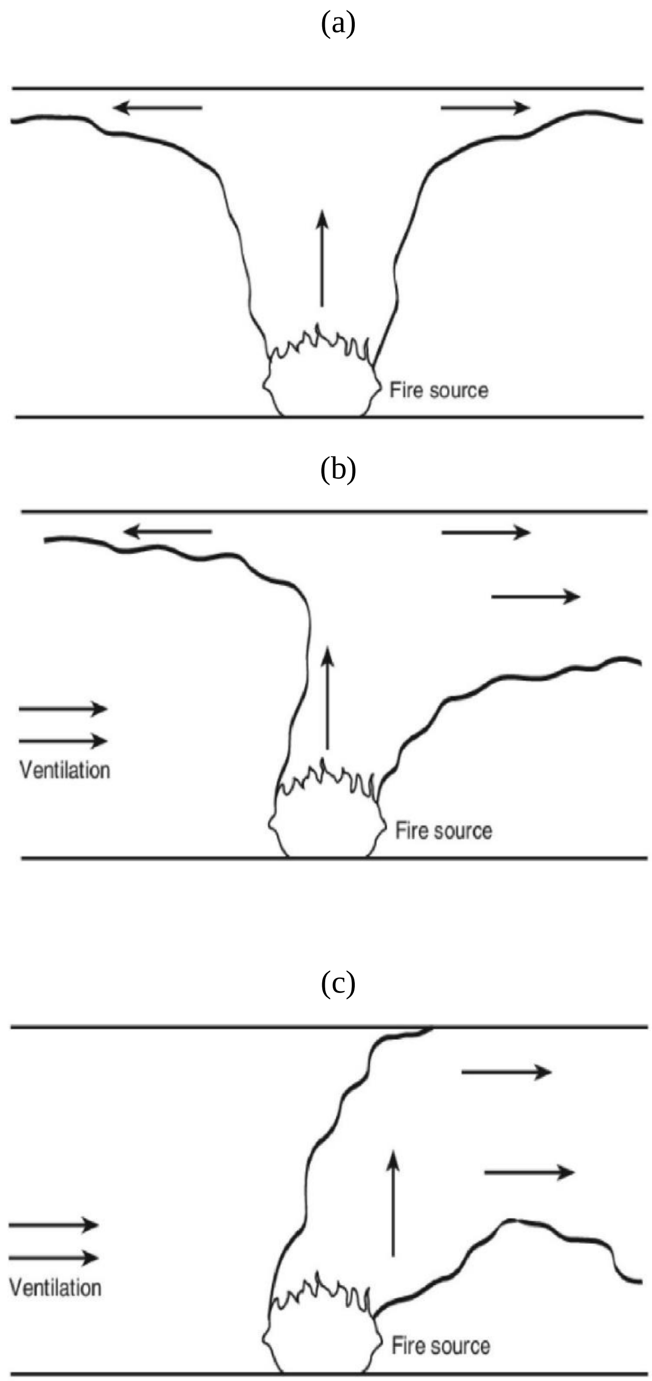

Figure 2.3. (a) Tunnel fire without ventilation (b) Insufficiently ventilated tunnel fire resulting in back-layering (c) Sufficiently ventilated tunnel fire to prevent back-layering [5]

2.4.2.1. Critical Froude number model

This model assumes full mixing between the ventilating air and the heat right at the fire site. The model was first proposed by Thomas [30, 31]. He suggested that critical ventilation velocity is achieved when the inertial force of the incoming air is equal to the buoyancy force of the smoke, i.e. the critical Froude number is unity, which results in

$$u_c = k\left(\frac{g\dot{Q}_C H}{\rho_o c_p T A}\right)^{1/3} \tag{2.13}$$

where u_c is the critical ventilation velocity in m/s, $\dot{Q}_C$ is the convective HRR in kW, c_p is the specific heat (kJ/ (kg K)), A is tunnel cross-sectional area (m^2), and T_o is the ambient temperature (K). Later, Danziger and Kennedy [32, 33] used the critical Froude number model and showed that the critical Froude number varies between 4.5 and 6.7 depending on the inclination of the tunnel. Also, they used average smoke temperature in the vicinity of the fire site in the correlation as shown in the following equations

$$u_c = k\left(\frac{g\dot{Q}_C H}{\rho_o c_p T_f A}\right)^{1/3} \tag{2.14}$$

$$T_f = \frac{\dot{Q}_C}{\rho_o c_p A u_c} + T_o \tag{2.15}$$

where the constant k is correlated with the critical Froude number by

$$k = {Fr_c}^{-1/3} \tag{2.16}$$

2.4.2.2. Oka and Atkinson's model

Oka and Atkinson [34] proposed the following equation for the critical ventilation velocity in a horseshoe shaped reduced tunnel model

$$u_c^* = \begin{cases} 0.7\, Q^{*1/3} & Q^* \le 0.124 \\ 0.35 & Q^* > 0.124 \end{cases} \tag{2.17}$$

where the dimensionless critical velocity and the dimensionless heat transfer are

$$u_c^* = \frac{u_c}{\sqrt{gH}} \quad , \quad Q^* = \frac{Q}{\rho_o c_p T_o g^{1/2} H^{5/2}}$$

2.4.2.3. Wu and Bakar's model

Wu and Bakar [35] carried out tests on a reduced scale tunnel model with aspects ratios between 0.5 and 4.0, and correlated the results with the hydraulic diameter of the tunnel by the using

$$u_{c,\overline{H}}^* = \begin{cases} 0.68\, Q_{\overline{H}}^{*1/3} & Q_{\overline{H}}{}^* \le 0.2 \\ 0.40 & Q_{\overline{H}}{}^* > 0.2 \end{cases} \tag{2.18}$$

where:

$$u_{c,\overline{H}}^* = \frac{u_c}{\sqrt{g\overline{H}}} \quad , \quad Q_{\overline{H}}^* = \frac{Q}{\rho_o c_p T_o g^{1/2} \overline{H}^{5/2}} \quad , \quad \overline{H} = 4\, A/P$$

2.4.2.4. Li et al.'s model

Li et al. [36] conducted tests in two scaled tunnel models and compared the results to a full-scale model and proposed the following equation

$$u_c^* = \begin{cases} 0.81\, Q^{*1/3} & Q^* \le 0.15 \\ 0.43 & Q^* > 0.15 \end{cases} \tag{2. 19}$$

where:

$$u_c^* = \frac{u_c}{\sqrt{gH}} \quad , \quad Q^* = \frac{Q}{\rho_o c_p T_o g^{1/2} H^{5/2}}$$

2.4.2.5. Li et al.'s corrected model

Again Li et al. [37] conducted numerical and theoretical work and proposed a new equation that accounts for tunnel width based on Li et al.'s model:

$$u_c^* = \begin{cases} 0.81\,\varphi^{-1/12}\,Q^{*1/3} & Q^* \le 0.15\,\varphi^{-1/4} \\ 0.43 & Q^* > 0.15\,\varphi^{-1/4} \end{cases} \tag{2.20}$$

where

$$u_c^* = \frac{u_c}{\sqrt{gH}} \quad , \quad Q^* = \frac{Q}{\rho_o c_p T_o g^{1/2} H^{5/2}} \quad , \quad \varphi = \frac{W}{H}$$

2.4.3. Turbulence intensity

In fluid dynamics, turbulent flow is defined as the flow whose motion is characterized by chaotic changes in velocity and pressure [38]. Turbulence intensity of a flow is defined as the ratio of root mean square velocity fluctuations (σ) to the mean velocity (ū), where η_i is a non-uniform weighting factor introduced to correct the velocity bias resulting from the high data rate and t_i is the residence of the i'th particle crossing the measurement volume [39].

$$Tu = \frac{\sigma}{\bar{u}}\,100\% \tag{2.21}$$

where

$$\bar{u} = \sum_{i=0}^{N-1} \eta_i u_i \quad , \quad \sigma = \sqrt{\sum_{i=0}^{N-1} \eta_i (u_i - \bar{u})^2} \quad , \quad \eta_i = \frac{t_i}{\sum_{i=0}^{N-1} t_j}$$

The importance of studying turbulence intensity in fire research is because it is related to oxygen availability of the fire which has significant effect on fire characteristics.

2.5. Studies on tunnel fires

Generally speaking, studies on tunnel fires can be divided in three groups: the large scale or full-scale experiments, the reduced scaled experiments and numerical modeling. Even though full-scale experiments are expected to give identical results to real fire incidents, yet, many reduced scale and numerical studies have also been conducted because they are easier to perform and offer the ability to control various parameters compared to full-scale experiments. Some of the major early full-scale experiments are the pool fire studies in railway tunnels in Glasgow and the FIRETUN project, which obtained a vast amount of HRR data for different vehicle fires [4, 40].

Later, a series of large-scale fire tests were performed as part of the Memorial Tunnel Fire Ventilation Program (MTFVTP) between 1993 and 1995 in USA [41]. In the test, Diesel pool fires were burned in 850 m long two-lane tunnel under different ventilation velocities. It was concluded that longitudinal ventilation velocity of 2.5-3 m/s was sufficient for smoke extraction of fires with HRR up to a maximum of 100 MW. To summarize the large-scale experiments, Ingason collected the HRR data from all the tests available in the literature before 2006 and normalized the peak heat release to the exposed fuel surface area [40]. He defined the fuel surface area as the freely exposed area where release of gasified fuel can occur simultaneously. Results are shown in Table 2.4.

Table 2.4. *Summary of normalized HRR for fire tests in tunnels [40]*

Type of fuel	Test series	Exposed fuel area (m^2)	Maximum heat release rate per square meter exposed fuel area MW/m^2
Liquid			
Gasoline	Ofenegg, Zwenberg, No.3 Shimizu	6.6, 47.5, 95	0.35 – 2.6
Kerosine	Glasgow	1.44	1.4
n-Heptane	Eureka	1, 3	3.5
n-60 % heptane/40% toulene	2nd Benelux	3.6, 7.2	1.1 – 1.6
Low-sulfur No 2 fuel oil	Memorial	4.5, 9, 22.2, 44.4	1.7 – 2.5
Solid fuel			
Wood cribs	Eureka (test 8, 9 and 10)	140	0.07 – 0.09
Wood pallets	2nd Benelux (tests 8, 9, 10 and 14)	120 (36 pallets) 240 (72 pallets)	0.11- 0.16
82 % wood pallets and 18 % PE pallets	Runehamar (test 1)	1200	0.17
82 % wood pallets and 18 % PUR matrasses	Runehamar (test 2)	630	0.25
81 % wood pallets and cartons and 19 % plastic cups	Runehamar (test 4)	160	0.44
HGV- furniture	Runehamar (test 3)	240	0.5
HGV- furniture	Eureka (test 21)	300	0.4
Vehicles			
Medium sized passenger cars	Assuming a 5 MW fire in the car	12 - 18	0.3 – 0.4
Passenger car plastic	Test 20 in Eureka	17 (no ceiling)	0.35
Buss	Test 7 in Eureka	80	0.36
Train	Test 11in Eureka	145	0.30
Subway coach	Test 14 in Eureka	130	0.27

* The heat of combustion of gasoline is assumed to be equal to 43.7 MJ/kg, 43.5 MJ/kg for kerosene, 44.6 MJ/kg for n-heptane.

Table 2.5 also represents a summary for important large-scale tunnel fire tests in the history of tunnel fire research and their respective results.

Table 2.5. *Summary of some large-scale tunnel fire experiments in literature [16]*

Test title	Year	Tunnel	Fire source	Main result
Glasgow experiments	1970	Disused railway tunnel	Kerosene pools	Smoke layers of 1-2 m advancing at 1-1.5 m/s speed
Zwenberg experiments	1976	Disused railway tunnel	Petrol and diesel pools	Ceiling temperatures as high as 1200 °C
EUREKA EU-499 test series	1990-92	Abandoned mine tunnel in Hammerfest	Cars, trains, carriages, heptane pools, and heavy good vehicles (HGV)	- Temperature of 800-900 °C during car fires and 1300 °C for HGVs. - Fire growth and burning pattern considerably affected by ventilation.
Memorial Tunnel Fire Ventilation Program	1993-95	Two lane road tunnel	diesel pool fires ranging in size (10-100 MW)	Considerable reduction in visibility due to smoke which posed a greater threat than fire heat load
Benelux experiments	2001	Operational tunnel	Pool fires, cars, a van and covered truck loads	High ventilation rates retarded development of car fire by up to 30 min but enhanced burning of HGV fires by up to 20 MW

In section 2.4.2, summary for various models to predict critical ventilation velocity were given. These models were based on experimental and numerical work on the reduced scale tunnel models. Oka and Atkinson investigated the effect of changes in the shape, size and location of the fire on the critical ventilation velocity [34]. The experiments took place in a 15 m long tunnel with 0.0569 m^2 cross section. The height of the tunnel was 24.4 cm and its width at the floor level was 27.4 cm with walls splayed out at 7° to the vertical as shown in Figure 2.4 (b). An orifice plate placed at the inlet provided a measure of the total volumetric flow. K-type thermocouples were planted in the upstream section to detect the upstream flow gases. The thermocouples were fixed 10 mm below the roof at distances of 1, 3, 5 and 10 tunnel heights upstream of the fire as shown in Figure 2.4 (b).

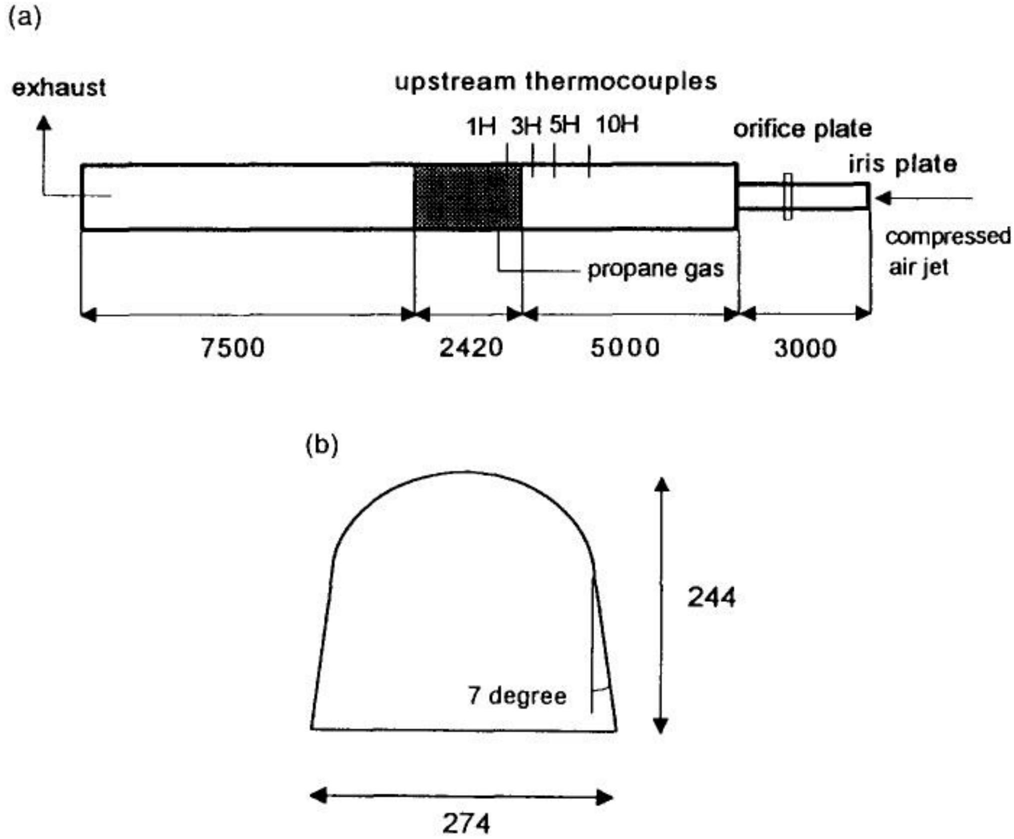

Figure 2.4. (a) Tunnel dimensions (b) Cross-section of the tunnel [34]

Propane gas was burned in the tunnel using burners of different sizes and at different locations. The volumetric flow rate is varied between 0.3 and 20 l/min. Using a scaling procedure described in that paper, the fire sizes correspond to fires of HRR between 2 and 150 MW in a tunnel that has a diameter around 5 m. For each burner, the critical velocity to prevent 'backing up' of the combustion products to 1, 3, 5 and tunnel heights was determined separately. Normalized dimensionless critical velocity against normalized heat released rate of this experiment were compared to full-scale data in Figure 2.5 at different backing up heights. In this thesis, critical velocity is defined as the velocity when the backlayering length is zero, which corresponds to the case when back-up distance is zero in Oka and Atkinson's work.

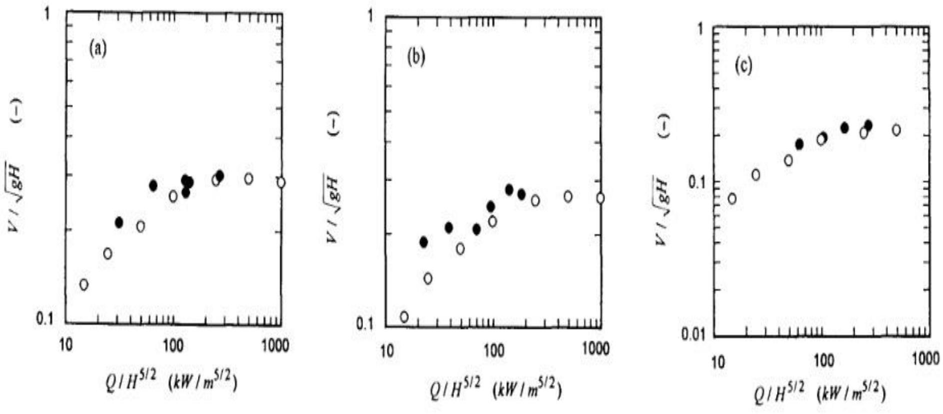

Figure 2.5. Dimensionless critical velocity vs normalized HRR, (●) full-scale tests; (○) model tests. The backing up distances for the plotted data are: (a) 1.4-4.5 tunnel heights for full-scale tests, 3 tunnel heights for model tests; (b) 4.5- 5.7 tunnel heights for full-scale tests, 5 tunnel heights for model tests; and (c) full-scale tests greater than 9 tunnel heights, model tests 10 tunnel heights [34]

Another empirical correlation for the critical ventilation velocity was proposed by Wu and Bakar [35]. They tried to study the effect of tunnel width on the critical ventilation velocity. They acquired detailed temperature and velocity distributions in five tunnels of the same height but different widths. Results showed that the critical ventilation velocity is independent of tunnel cross-section. The experimental setups were almost the same as the one used by Oka and Atkinson except that they used different tunnel cross-sections. The tunnel was 15 m long with K-type thermocouples distributed identical to the one used by Oka and Atkinson. Again, propane gas as fuel source with fire sizes corresponding to fires of approximately 2.5-50 MW HRR in a tunnel having a diameter of around 5 m. Ventilation velocity was controlled using the orifice plate similar to Oka and Atkinson's model. Three more arrays of 8 K -type thermocouples were used to determine temperature distribution in near fire zone and downstream of the fire.

After normalizing the results of critical ventilation velocity against HRR, Figure 2.6, but this time using the hydraulic diameter as the characteristic length, not the tunnel height as in Oka and Atkinson's model, it can be noticed that all the experimental results can be corelated into a single form. Using those results, Wu and Bakar proposed equation (2.18).

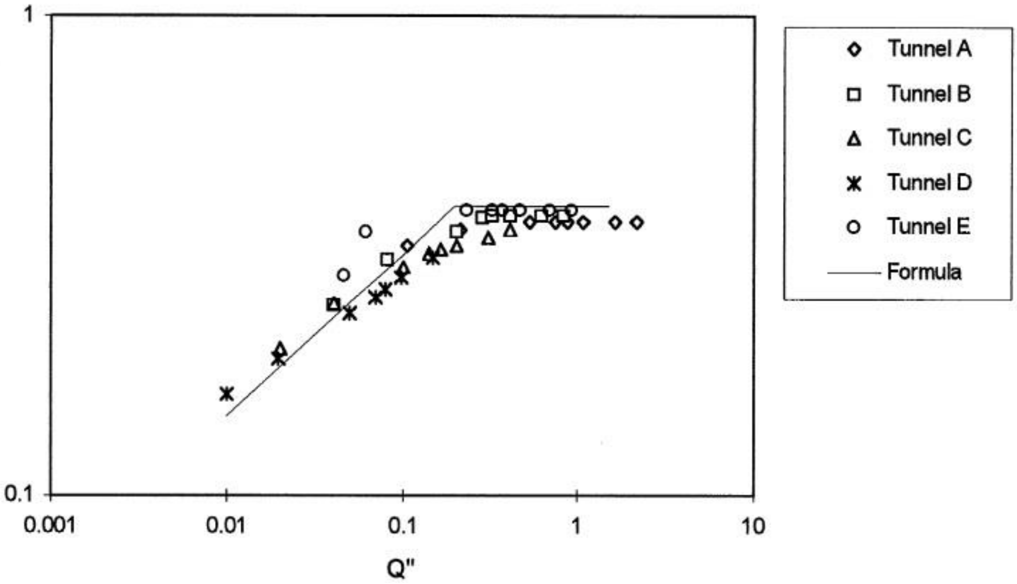

Figure 2.6. Dimensionless critical velocity against dimensionless heat release rate [35]

Li et al. conducted experimental tests and theoretical analyses to investigate the critical velocity together with the backlayering length [36]. In this work, two longitudinally ventilated model tunnels were used. Both tunnels were 12 m long having 5.25 m long air supply duct with a static pressure box to smooth the turbulence of the air flow.

In tunnel A, a 100 mm diameter porous bed burner was used as a fire source, and a 150 mm diameter burner was used in tunnel B. Propane was used as burning fuel, and its flow rate was measured using a rotameter. Ventilation flow rate was measured by a vortex flowmeter with a range of 3-540 m^3/h. K-type thermocouples of 1.0 mm diameter were mounted 10 mm below the center line of the ceiling to measure gas temperature. After a series of experiments in tunnels A and B, model car was placed inside tunnel B to study the effect of blockage on the critical velocity and back-layering length.

Experimental results are shown in Figure 2.7. It can be noticed that similar to Wu and Bakar's and Oka and Atkinson's models, dimensionless velocity has two regimes, one is dependent on HRR and the other is not when Q^* is larger than 0.15. Results also show that Wu and Bakar's model gave lower critical velocity values especially when Q^* is less than 0.15. Correlation is given by equation (2.19).

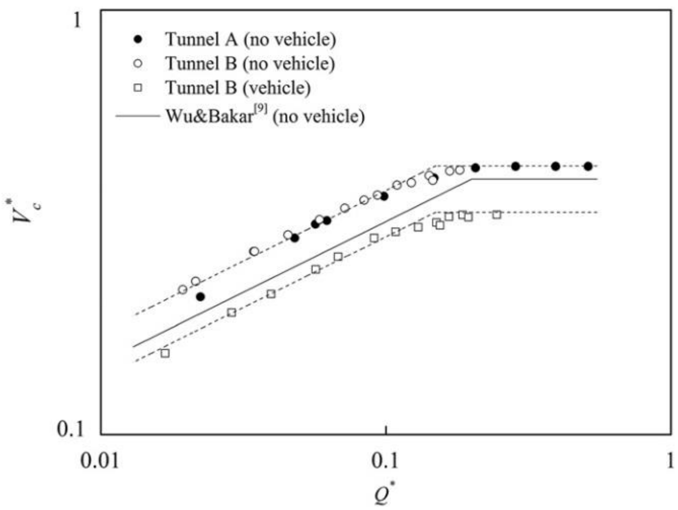

Figure 2.7. Variation of dimensionless critical velocity against dimensionless HRR [36]

Another work of Li et al. studied the effect of tunnel cross-section on critical velocity by conducting numerical and theoretical analyses [37]. FDS 6.2 was used to carry out six series of simulation, one series simulated the model scale fire and the other five series simulated the full-scale fires. The model scale tunnel simulated was the one used in [36] with a fire source of 0.1 m x 0.1 m placed at the center of the tunnel. The simulated full-scale tunnels were 5 m high and 100 long with a 2 m x 2 m fire source placed at the center of the tunnel. Widths of tunnels were 5 m, 10 m, 15 m and 30 m (aspect ratios are 1, 2, 3 and 6). LES model was used to model turbulence. Results of the study led to correct equation (2.19) for the width of tunnel, and equation (2.20) was proposed.

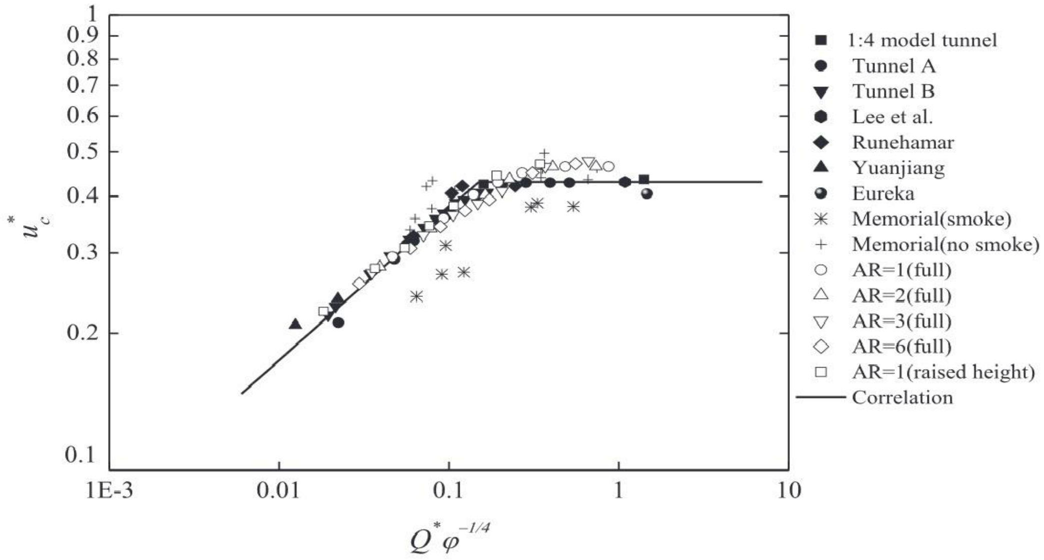

Figure 2.8. Test data and numerical results compared to correlation [37]

2.6. Previous studies conducted using the experimental setup

The experimental setup was used in conducting other studies before the renovation in current work. Kayili et al. investigated the effect of blockage ratio (the ratio of the model cross sectional area to the tunnel cross sectional area) on HRR and temperature distribution using the previous setup [42]. Square based model vehicles were built according to a theory available in the literature called wood crib theory. Wood cribs of different sizes were burnt at four different ventilation velocities (0.5, 1, 2 and 3 m/s). Temperature distribution was measured using K-type thermocouples of 0.5 mm diameter.

HRR was calculated using the Oxygen Consumption Calorimetry Method discussed previously in section 2.4.1. The study concluded that HRR increases with increasing blockage ratio. It also concluded that temperature values inside tunnel increase with the increase of ventilation velocity up a certain value, further increase in ventilation velocity will cause temperature values to drop as the cooling effect of ventilation takes over and HRR starts to decrease. Figure 2.9 shows typical experimental results from [42]. Again, Kayili et al. investigated the blockage effect on HRR in [43] and it was concluded that 79.8% of the variation in heat release rate is attributed to changes in blockage ratio,10.6% to changes in thickness, and 4.5% to changes in velocity.

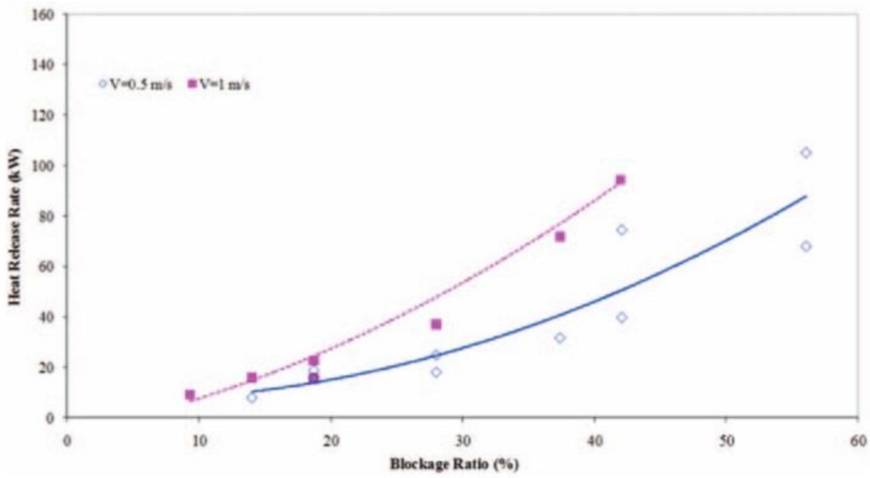

Figure 2.9. HRR vs blockage ratio for velocities of 0.5 and 1 m/s [42]

The tunnel model was modified and used in a series of experiments to investigate the effects of interacting fires on the burning rate and HRR in tunnel fires [14]. In this study, ethanol square pool fires of 10 and 15 cm size were burnt in the model tunnel. Experiments included the single and dual pool fire scenarios. Figure 2.10 shows that for dual pools burning duration is shorter than that for single pools. It was shown that the burning rate of interacting pool fires was 2.3 times that of single fire cases. Figure 2.11 compares the burning rates of single pool (SP) and dual pools (DP) fires as a function of pool depth at different ventilation velocities. It was seen that increasing the ventilation velocity had a steady enhancing effect on the burning rates of 10 cm pool cases, but for 15 cm pool fires the effect was nonlinear.

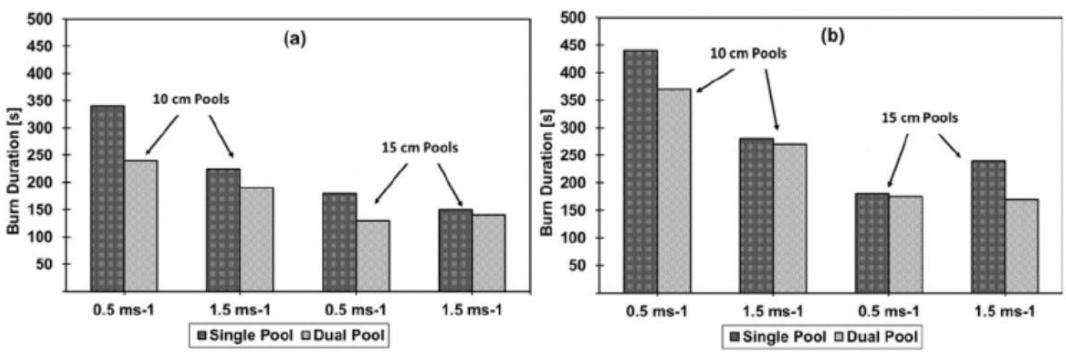

Figure 2.10. Burn duration of SP and DP fires as a function of ventilation velocity for initial fuel mass of (a)40 g and (b) 80 g [14]

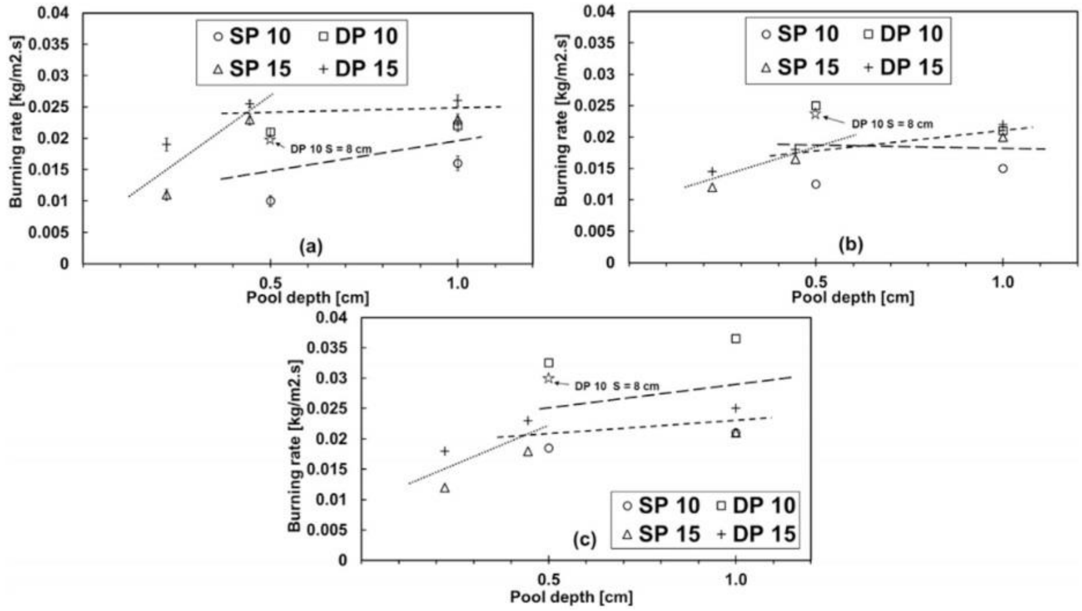

Figure 2.11. Burning rates of SP and DP fires as a function of pool depth (a) 0.5 m/s (b) 1 m/s (c) 1.5 m/s. [14]

In the most recent work on the setup, Shafee and Yozgatlıgil studied the effect of tunnel blockage and tunnel inclination on burning rate, HRR and smoke backlayering [44]. In this study, ethanol was again used as the fuel source and burning rate and temperature values were measured. Tunnel cross-sectional area blockage ratio was tested under three cases of no blockage, 14% and 56%. The grade of inclination of tunnel was varied between -6% uphill and +3% downhill. Results in Figures 2.12 and 2.13 show that HRR and maximum ceiling temperature increase in the downhill case. Results also showed that critical velocity decreased when moving to uphill inclined cases. A statistical model was applied on the results showed that ventilation velocity is the main factor contributing to the HRR with 45%, blockage at 25%, and inclination at 19%.

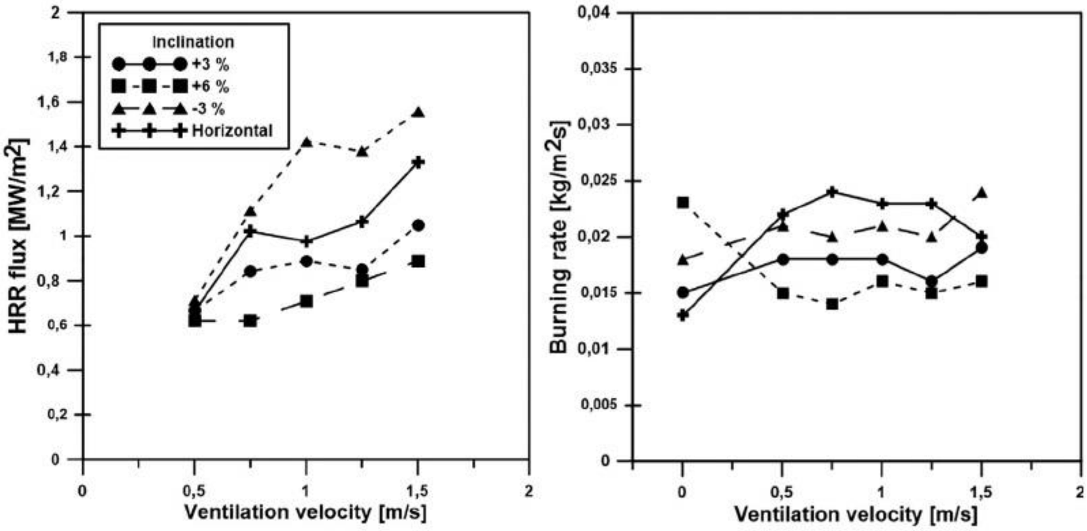

Figure 2.12. Effect of tunnel inclination on the burning rates HRR flux from fires [44]

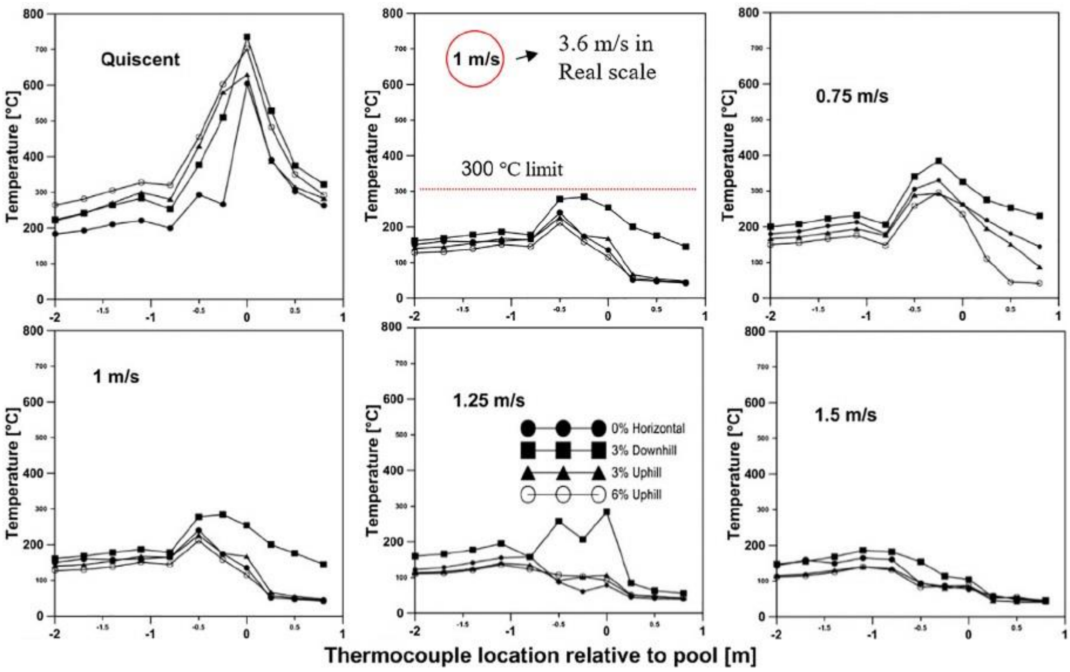

Figure 2.13. Effect of tunnel inclination on the maximum ceiling temperatures as a function of ventilation velocity and inclination grade [44]

CHAPTER 3

EXPERIMENTAL SETUP AND INSTRUMENTATION

3.1. The pre-renovation experimental setup

The experimental setup was constructed based on Froude scaling and represents a bored underground metro tunnel in Istanbul, Turkey. The cross-sectional area of the real scale tunnel is 20.75m^2 and diameter of 5.2 m [42, 43]. The cross-section of the reduced scale model has an arched ceiling of 20 cm radius and rectangular base of 40 cm width and 16.4 cm height as shown in Figure 3.1. The length of the scaled model is approximately 10 m including the chimney section.

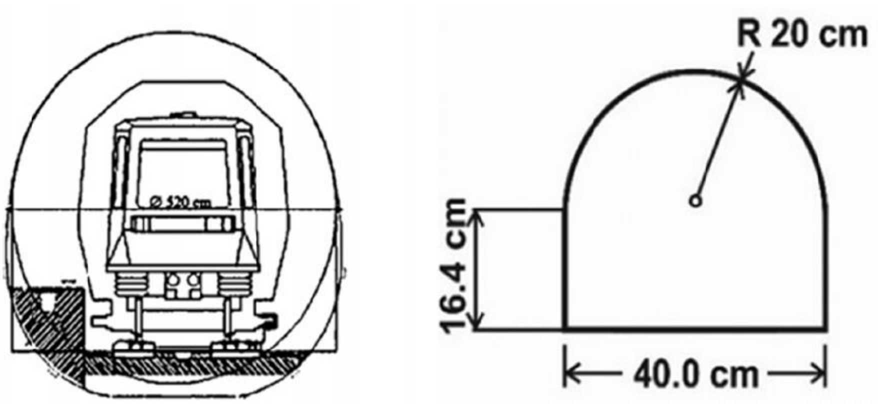

Figure 3.1. Schematics of the real and model cross section [43]

Before renovating the tunnel model, it was located outside the Fluid Mechanics Laboratory of Middle East Technical University. The model was composed of an axial compressor, which supplied laboratory air as the longitudinal ventilation to the tunnel model. This compressor was controlled by a speed-controlled motor that was connected to a compressor intake as shown in Figure 3.2. The supplied air then passed through a plenum that dampened the airflow. All the previously mentioned components, the compressor and the plenum, were placed inside the lab. The plenum was connected to an L-shaped channel that passed the air to the model tunnel located outside the lab as shown in Figure 3.3.

Figure 3.2. The compressor of the previous setup

Figure 3.3. The L-shaped connecting channel

Then, airflow passed through a flow straightener before entering the upstream section of the tunnel, Figure 3.4. The tunnel is composed of 1.5 m upstream section, 1.5 m combustion section where the fire experiments are conduced, a 4.5 m downstream section of three connected modules and a chimney section. Figure 3.5 shows the modules and the chimney section outside the lab.

Figure 3.4. The flow straightener

Figure 3.5. Tunnel modules and the chimney section in the previous model [16]

The velocity of the airflow was measured by hotwire anemometer in the upstream of fire during previous experiments by traversing the probe at 5 cm height intervals at the center of the tunnel cross section. The readings of the anemometer were recorded with 0.2 Hz frequency over 600 s period while the compressor was operated at specified speed within the range between 0.5 and 2.5 m/s [16]. Figure 3.6 shows a schematic drawing for the previous setup. A total of 27 K-type thermocouples were implemented along the tunnel as shown in Figure 3.7 [43].

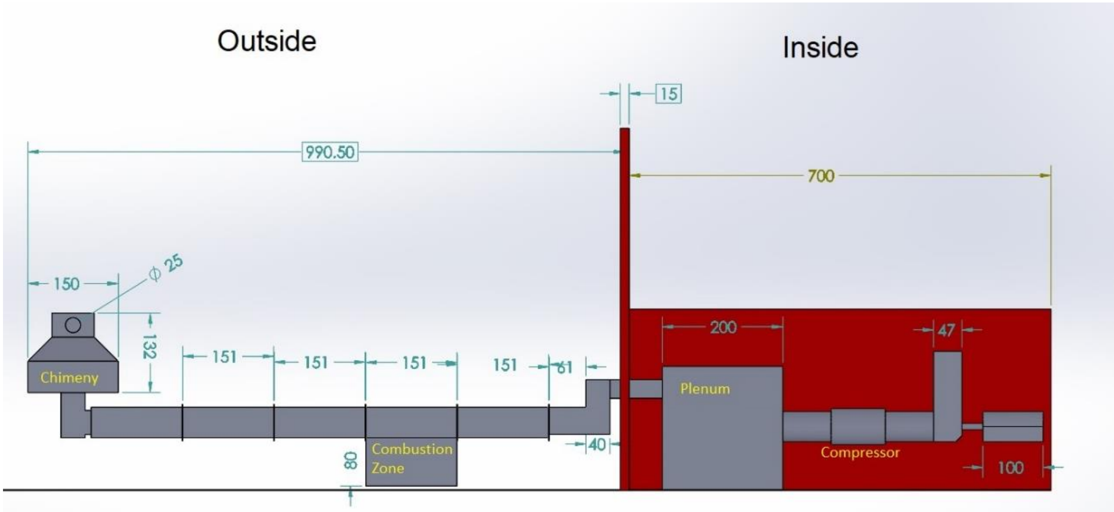

Figure 3.6. Schematic drawing of the previous experimental setup

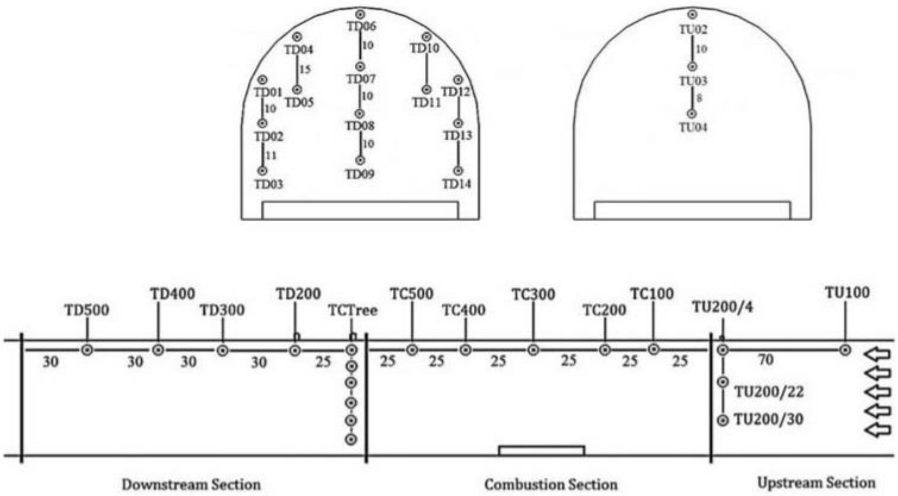

Figure 3.7. Thermocouple indicators and configuration along the previous scaled tunnel

3.2. Renovation of the experimental setup

Even though the studies conducted using the previous experimental setup gave results that agreed well with other works in the literature, yet, the setup was renovated to improve the accuracy and control of experiment parameters while adding new equipment to characterize the tunnel flow which was not conducted before. Therefore, the motivations to rectify the previous tunnel model can be summarized as follows:

- Adding a transparent section for flow characterization using LDA method. This also allows understanding the mutual effect between ventilation flow and HRR of the fire. See Figure 3.8

Figure 3.8. The transparent section used to make LDA measurements

- Relocation of the experimental setup for better controlled environment to eliminate the effect of the surroundings. By doing this, experiments would also be more accurate.

The renovation started by dismantling the five modules, then the metal sheets, old thermocouples and the old insulation material were removed and discarded as shown in Figure 3.9. Later, the legs that carried the modules were trimmed as shown in Figure 3.10.

Figure 3.9. Dismantled modules after removing the metal sheets and the old insulation

Figure 3.10. The modules after trimming the legs

In order to facilitate the mobility of the modules for any future adjustments or changes, three steel foundations were designed to carry the modules without the need of welding or joining, a technical drawing of the foundations is shown in Figure 3.11. The modules were covered with a new insulation material, Figure 3.12, painted, covered with new metal sheets except the top, to add new thermocouples, and placed on the foundations, Figure 3.13.

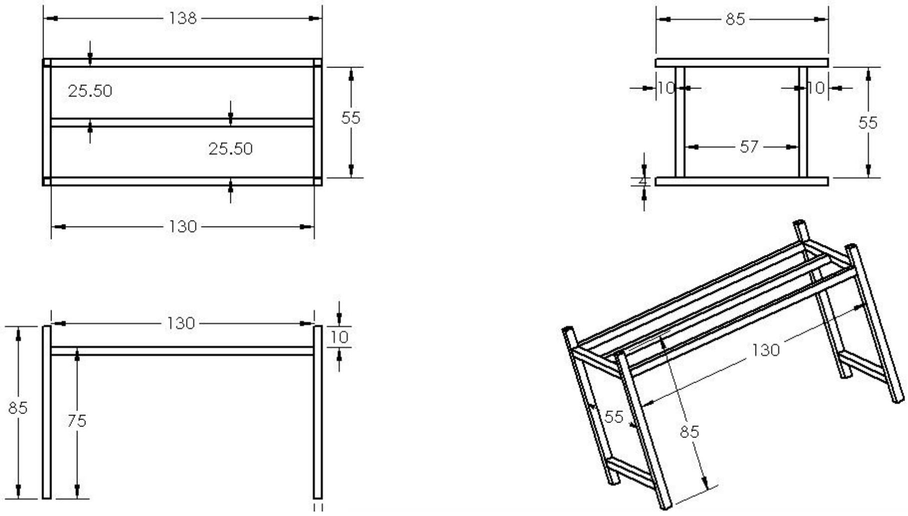

Figure 3.11. Technical drawing of the foundations

Figure 3.12. New insulation wrapped around the modules

Figure 3.13. A module covered with metal sheets except the top

After that, new series of K-type thermocouples were mounted inside the modules and the tops of the modules were covered as shown in Figure 3.14.

Figure 3.14. A module after planting thermocouple and covering the top

As it was mentioned before, flow characterization was planned to be conducted using LDA technique which needs the flow to pass through a transparent channel, so a transparent glass part with horseshoe shape was made, the transparent section has similar shape as the cross-section of the tunnel but having few millimeters smaller dimensions so it can be placed inside the tunnel. The airflow is generated using a blower type fan connected to a damping section as shown in Figure 3.16. The damping section was composed of a coarse doormat material placed inside a steel container as shown in Figure 3.17. The damper was carried using a foundation like the ones carrying the modules. A flow straightener was placed at the end of the damping section as shown in Figure 3.18, and the damper was connected to the transparent section. Figure 3.19 shows the final configuration of the upstream section after connecting the fan and the transparent glass to the upstream module.

Figure 3.15. Transparent glass after attaching it to the upstream

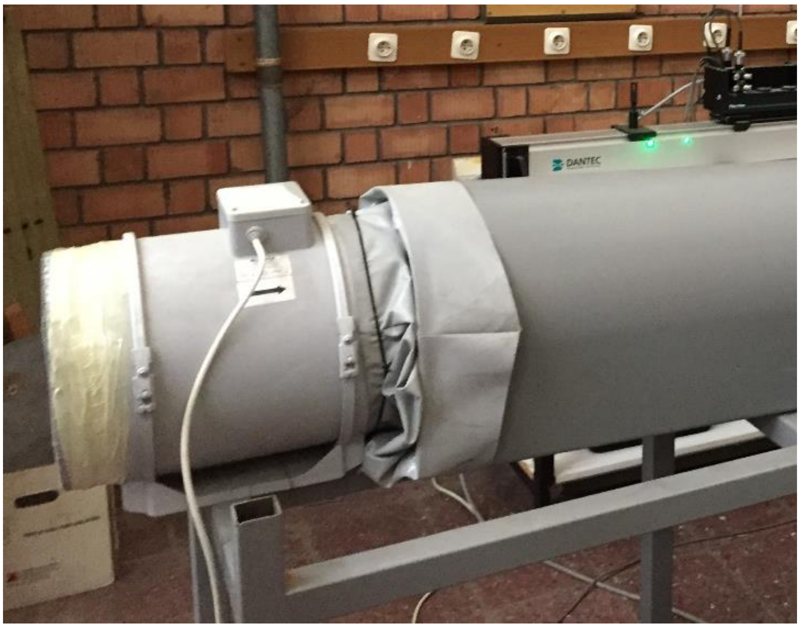

Figure 3.16. The fan connected to the damper

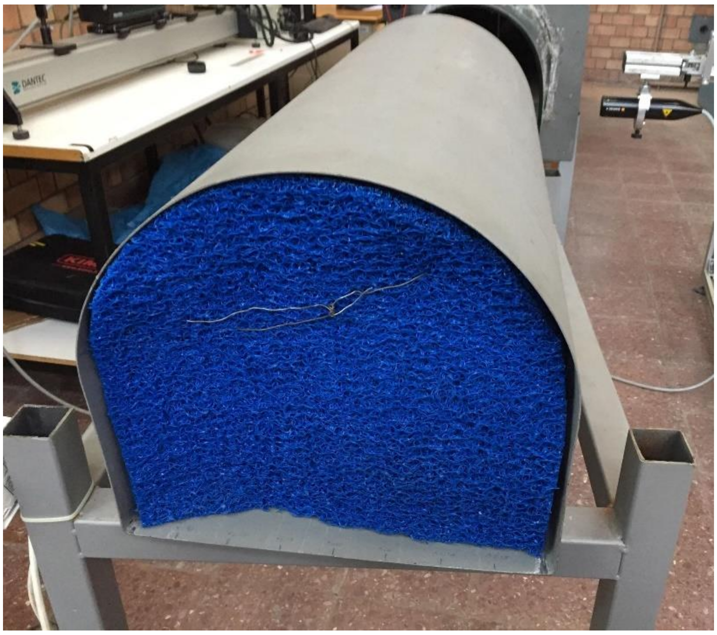

Figure 3.17. Coarse doormat placed inside the damper

Figure 3.18. The honeycomb flow straightener placed inside the damper

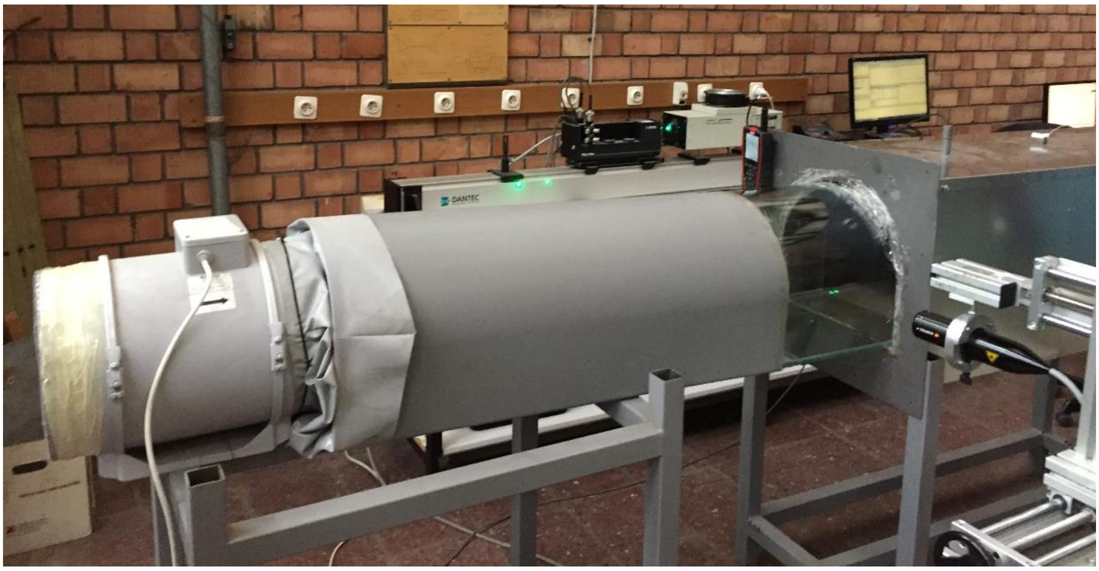

Figure 3.19. Final configuration of the upstream section

Later, a hole was drilled through the wall of the lab. In the new setup, the upstream module (US) and two of the downstream modules (D1 and D3) were carried by the new foundations, while the combustion zone (CZ) was carried by the bolts that connecting it to US and D1. US, CZ and D1 modules were placed inside the lab while D3 was outside, D2 module was placed through the hole drilled in the wall of the lab as shown in Figure 3.20. The modules were connected to each other using bolts and nuts with pieces of wick in between to prevent air leakage, Figure 3.21, and D3 was connected to the chimney as shown in Figure 3.22. Figure 3.23 shows a schematic drawing of the whole setup after renovation.

Figure 3.20. Downstream 2 module passes through the hole

Figure 3.21. Band of wick between modules to prevent leakage

Figure 3.22. Downstream 3 module connected to the chimney outside the lab

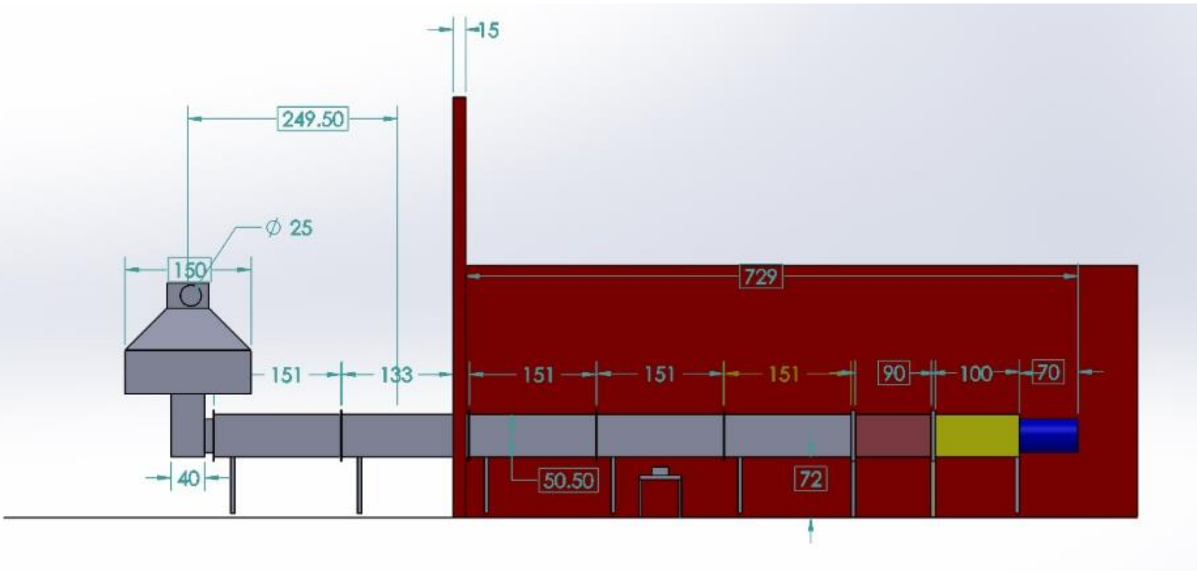

Figure 3.23. Schematic drawing of the setup after renovation

3.3. Instruments

3.3.1. Flow characterization

For flow characterization, Laser Doppler Anemometry (LDA) technique was employed. LDA is a non-intrusive measuring technique invented by Yeh and Cummins in 1964 [45]. This technique is a pointwise velocity measurement technique that can be used to measure up to 3 velocity components in both gaseous and liquid flows at very high accuracy. LDA is widely used in different applications such as aerodynamics and hydrodynamics, combustion studies and velocity and vibration measurements on surfaces, because it can be used to measure velocity in laminar, turbulent, subsonic, supersonic, hot and cold flows. The working principle of LDA is pointing focused laser beams to intersect at the point of interest to form a measurement volume as seen in Figure 3.24 [46]. Tracing particles are being fed to the system, and when a tracing particle passes through the measurement volume backscattered light is formed, this scattered light has components from both beams. Those two components interfere on the surface of a photodetector. Since the particle is moving inside the volume, the interference produces pulsating light intensity due to changes in the difference between the optical path lengths of the two components, then the signal processing takes place in the spectrum analyzer to convert the frequency to velocity measurement. Figure 3.25 shows the working principle of the LDA. For more information about LDA working principles [47, 48]. In this work, Sky Walker fog generator was used, and ST-Smoke Fluid High was used as seeding material.

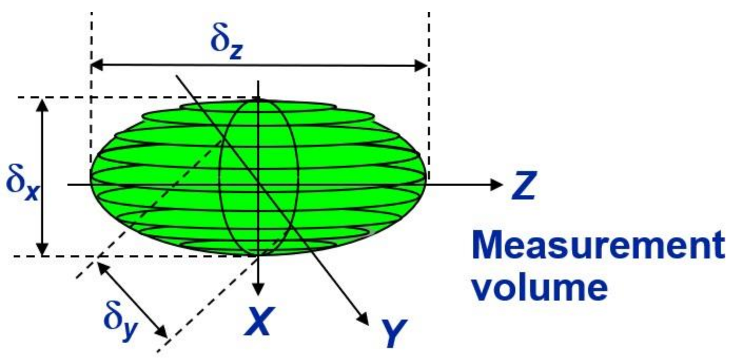

Figure 3.24. LDA measurement volume [46]

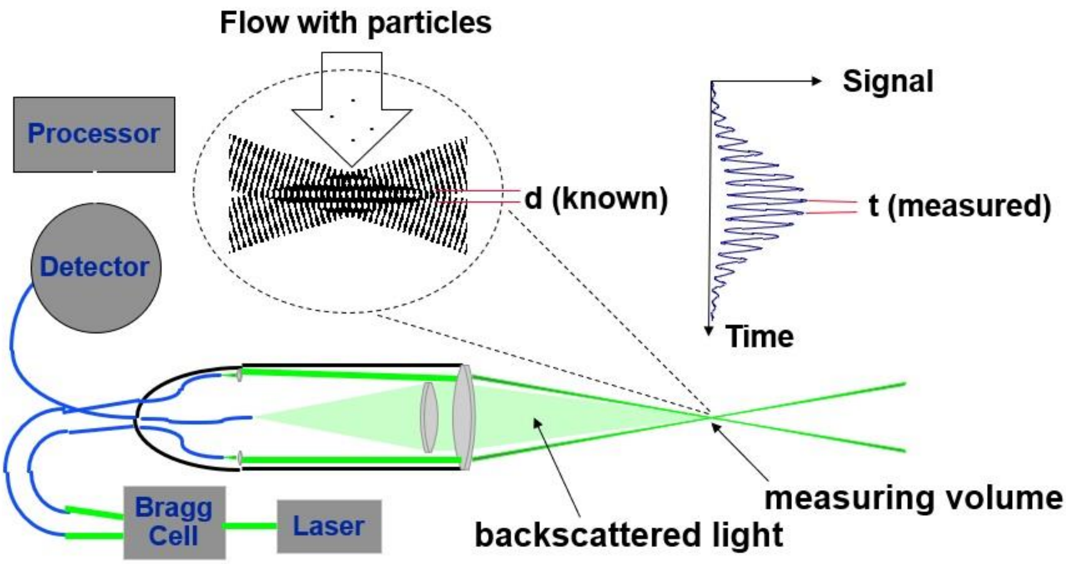

Figure 3.25. LDA working principle [46]

3.3.2. Gas temperature

New series of K-type thermocouples were implemented in the tunnel model for measuring temperatures throughout the tunnel with more even distribution for better measurement. K-type thermocouples were chosen due their high accuracy and wide temperature range in addition to their inexpensive price. The temperature range of K-type thermocouples is -270 to 1260 °C with +/- 0.75% accuracy [49]. Figure 3.26 shows the distribution of thermocouples inside the tunnel. The tree configuration at the beginning of the downstream aims to give a way to visualize the shape of the smoke cloud across the tunnel. The data provided by thermocouples on the upstream give an idea about the length and thickness of the backlayering. The maximum temperature is expected to be in the combustion zone for most of the scenarios so five couples of thermocouples were planted in the combustion zone with 25 cm distance between each. The TC209/20 stands for the thermocouple that is connected to channel 209 in the data logger which is 20 cm below the ceiling of the tunnel.

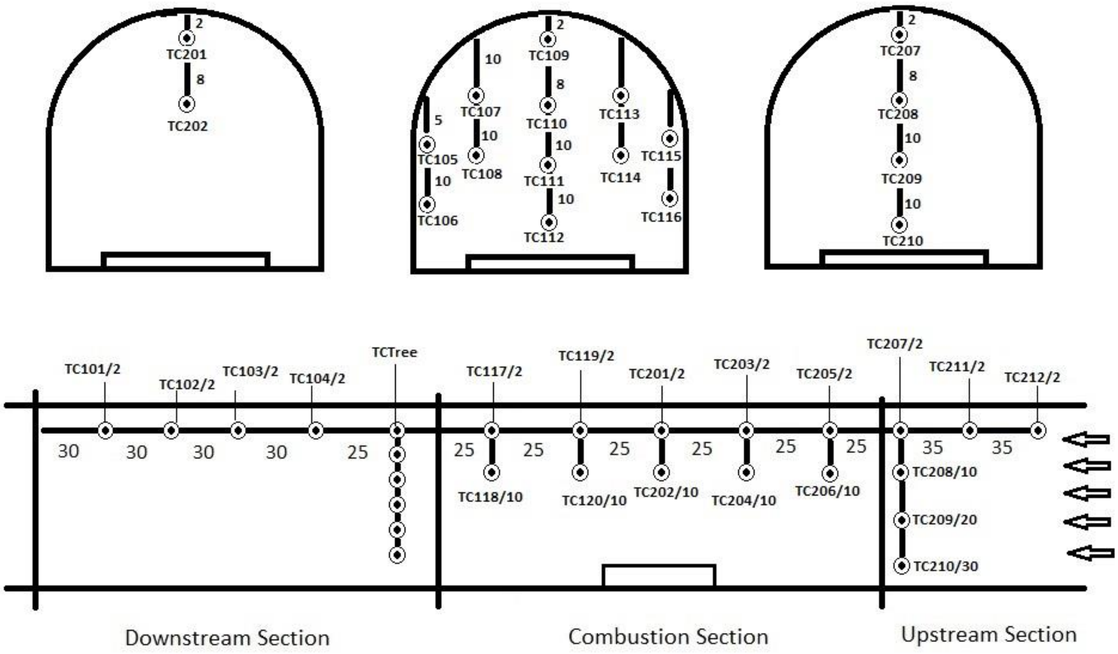

Figure 3.26. Thermocouple indicators and configuration along the scaled tunnel

Agilent 34972A Data Acquisition Unit was used to log the data provided by the thermocouples. Thermocouples were connected to two data loggers with 20 channels each, the data loggers are connected to the acquisition unit which is placed above the combustion zone. Agilent 34972A Data Logger provides an accuracy of +/-1.5 °C.

3.3.3. Burning rate

Burning rate was defined as mass loss rate of fire per unit. MLR was obtained using the derivative of mass loss history. The mass loss history was measured using RADWAG 25-R2 load cell with internal stability feature and readability of 10 mg at a sampling frequency of 5 Hz and a linearity of ±20 mg. The load cell was connected to a computer and mass loss history was recorded using a specific software. The burning rate and mass loss rate were calculated using the following equations

$$BR = \frac{dm_{fu}/dt}{A_{Burned}} \tag{3.1}$$

$$-\left(\frac{dm_{fu}}{dt}\right)_i = \frac{m_i - m_{i+1}}{\Delta t} \tag{3.2}$$

The uncertainty of burning rate measurements using this method was demonstrated to be ±5% [14]. A typical mass history and a burning rate history are shown in Figure 3.27.

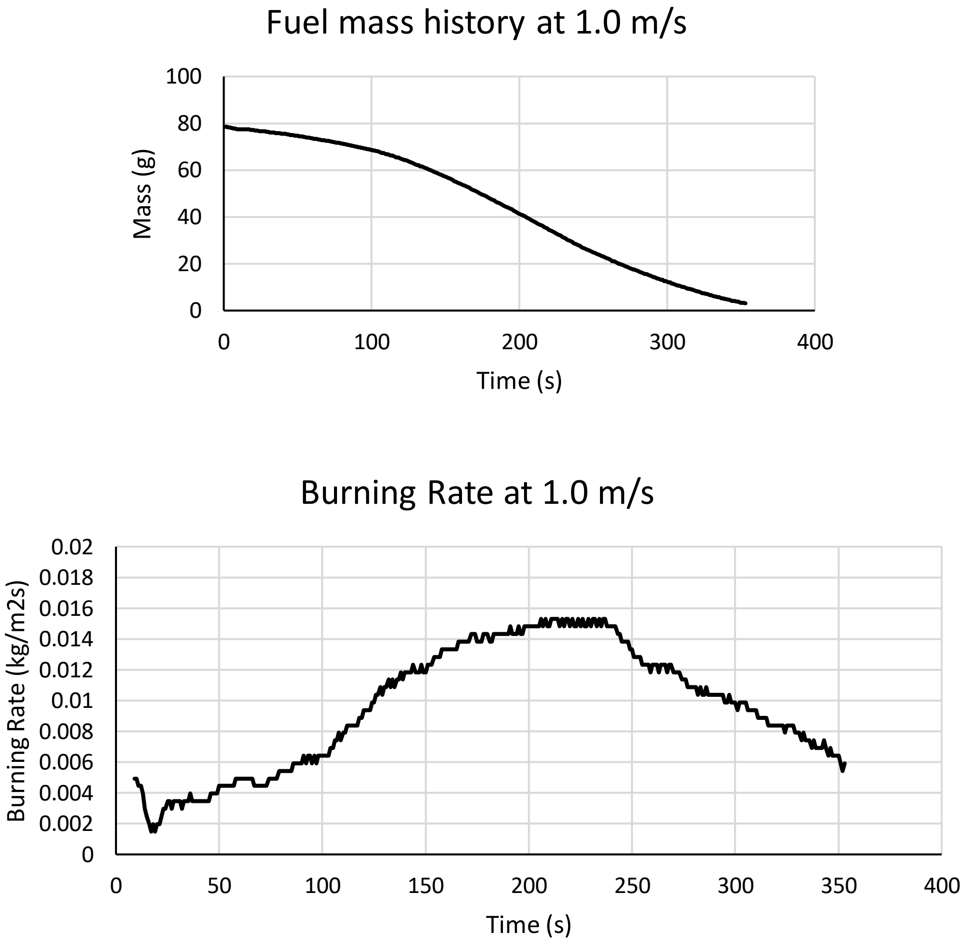

Figure 3.27. Typical mass loss history and calculated burning rate from experiments

CHAPTER 4

EXPERIMENTAL METHODS

4.1. Tunnel characterization

The LDA laser probe was attached to a traverse system to the right of the transparent section of the tunnel as shown in Figure 4.1. This system allowed traversing the laser beams in three directions to measure the flow velocity at the point of interest within the cross-section of the transparent glass. Tunnel flow characterization was done at three ventilation velocities, 0.5 m/s, 1.0 m/s and 1.5 m/s. A hotwire flow anemometer was also placed in the upstream module at a height of 15 cm (i.e. middle of the tunnel cross-section) to be able to compare the results with LDA measurements. The fan speed was adjusted until the desired ventilation velocity was read by the LDA at the same place as the hotwire, height of 15 cm at the centerline of the tunnel. Then the smoke generator was turned on to supply tracing particles inside the tunnel while the laser beams were pointing at the point of interest. Measurements were taken at 24 locations in the tunnel cross-section as shown in Figure 4.2 and a side view of the measurement locations is shown in Figure 4.3. Data points were measured along the centerline of the tunnel at different heights with 5 cm intervals, and below the curvature of the glass. At heights of 5 cm, 10 cm and 15 cm, more data points were taken to visualize the horizontal velocity profile along the tunnel.

Figure 4.1. The traverse system

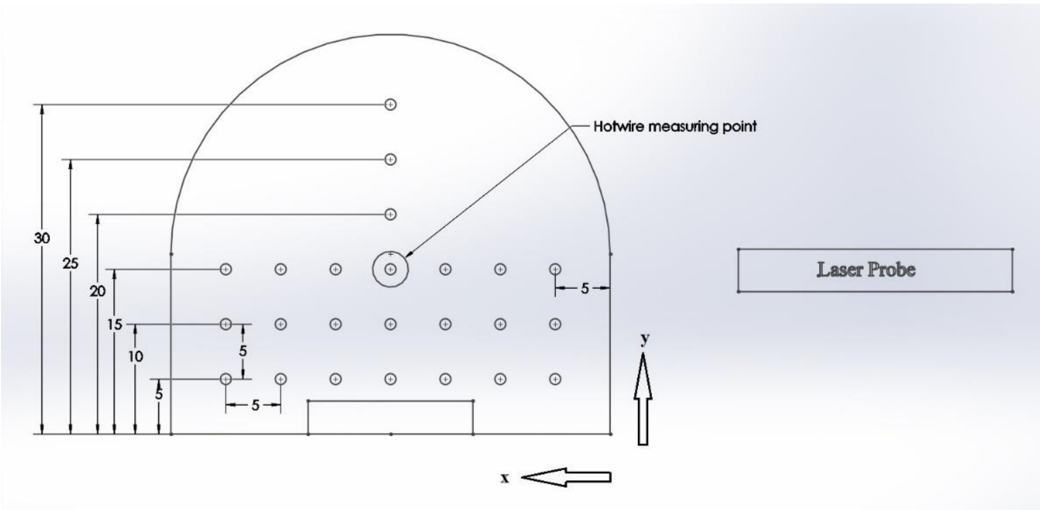

Figure 4.2. Locations of the measuring points

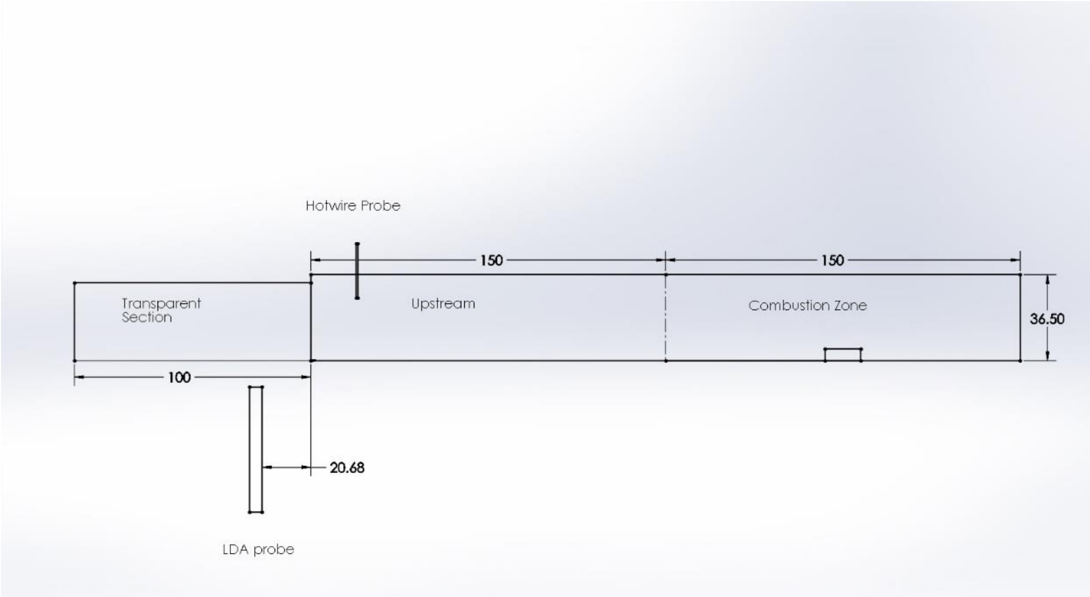

Figure 4.3. Side view of the tunnel showing measurements locations

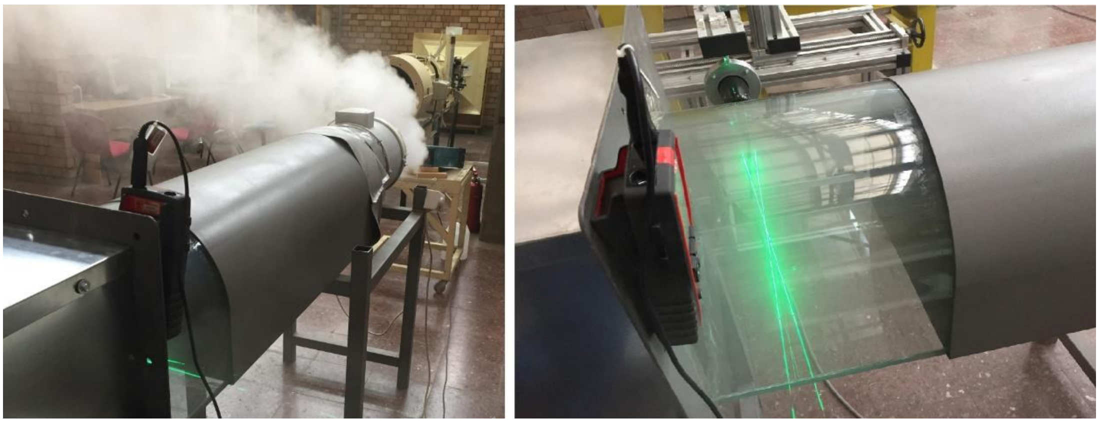

Figure 4.4. Typical flow velocity measurement test using LDA

Results of tunnel characterization are presented and discussed in section 5.1.

4.2. Pool fires

In literature, fire is simulated using different methods. Some studies use biomass fuels [50, 51] such as wood, while others use gaseous fuel supply such as propane [18]; but the most commonly used method is liquid pool fuels due to their easier handling [52, 53, 54, 55, 56, 57]. The most commonly used fuels are diesel, heptane and ethanol. In this work, 100 ml ethanol pool fires are used in all test cases for simulating fire sources. The pool fires were conducted at the center of the combustion zone along the longitudinal axis of the tunnel. A 15 cm square fuel tray was used as the pool container as shown in Figure 4.5. The thermo-physical properties of ethanol used in the experiments are given in Table 4.1 [14].

Table 4.1 *Ethanol fuel properties*

Molar mass (g/mol)	Density (g/cm^3)	Boiling point ($^{\circ}C$)	Specific heat (J/mol. K)	Heat of combustion (kJ/mol)
46.07	0.79	78.4	112.4	1365

Figure 4.5. Fuel tray (15 cm square pool)

4.3. Experimental procedure

The repeatability of the fire experiments can be affected depending on the season the experiments when conducted in an open area. To overcome this problem, the tunnel was relocated inside the Fluid Mechanics Laboratory of the Mechanical Engineering Department of Middle East Technical University. Only the chimney section of the previous setup remained outside due to safety reasons. In the renovated model, the ambient temperature was more or less constant in the laboratory throughout the year and there was no draft effect from the surroundings. Before conducting the hot flow experiments, a warm up test was made by burning some amount fuel to insure uniform pan and tunnel ambient temperature conditions before conducting the succeeding experiments. Then fan speed was adjusted until the LDA reads the desired value, e.g. 0.75 m/s, at the height of 15 cm and the load cell reading was reset to zero. Temperature and fuel mass data logging were started right before igniting the pool fire. Mass history was recorded until all the ethanol in the tray is burnt, while temperature recording was continued until the tunnel cools down. Then the fan was adjusted to the new ventilation velocity and the procedure was repeated for all test cases.

4.4. Experimental matrix

Table 4.2 shows the experimental matrix for the study. Cold flow tunnel characterization was performed at ventilation velocities of 0.5, 1.0 and 1.5 m/s which correspond to low, medium and high limits of ventilation applied in the study. MLR is recorded for hot flow experiments between 0.25 and 1.75 m/s with 0.25 m/s velocity increment. HRR is calculated from the MLR data as was discussed in section 2.4.1. Temperature distribution is recorded in all experiments. The 0.8 m/s and 0.85 m/s cases where conducted to find the exact critical ventilation velocity value for which details are given in section 5.4.

Table 4.2. *Experimental matrix for hot and cold flow experiments*

Exp. No.	Flow mode	Longitudinal Ventilation Velocity	LDA Measurement Points	Parameters to be measured
1	Cold Flow	0.5	24	Flow Velocity
2	Cold Flow	1.0	24	Flow Velocity
3	Cold Flow	1.5	24	Flow Velocity
4	With Combustion	0.25	0	Temperature, MLR, HRR
5	With Combustion	0.35	3	Flow Velocity, Temperature
6	With Combustion	0.4	3	Flow Velocity, Temperature
7	With Combustion	0.45	3	Flow Velocity, Temperature
8	With Combustion	0.5	3	Flow Velocity, Temperature, MLR, HRR
9	With Combustion	0.55	3	Flow Velocity, Temperature
10	With Combustion	0.75	3	Flow Velocity, Temperature, MLR, HRR
11	With Combustion	0.8	3	Flow Velocity, Temperature, MLR, HRR
12	With Combustion	0.85	3	Flow Velocity, Temperature, MLR, HRR
13	With Combustion	1.0	3	Flow Velocity, Temperature, MLR, HRR
14	With Combustion	1.25	3	Flow Velocity, Temperature, MLR, HRR
15	With Combustion	1.5	3	Flow Velocity, Temperature, MLR, HRR
16	With Combustion	1.75	3	Flow Velocity, Temperature, MLR, HRR
	Total Number of Experiments			40

CHAPTER 5

RESULTS AND DISCUSSION

5.1. Tunnel characterization results

There have been numerous studies in literature studying the effect of ventilation velocity on pool fires, yet, there has been no major work discussing the effect of fire on flow field in the upstream of the tunnel. In most of the studies that discuss tunnel fires, flow velocity is measured using hotwire anemometers at the middle of the cross-section assuming that the velocity is uniform [58, 59, 60]. In most of the reduced-scale tunnel studies, either a plenum or a diffuser is used to obtain a uniform velocity profile inside the tunnel, but the accuracy of the hotwire reading is questionable. In this study, a blower type fan was used to supply airflow inside the tunnel, the air passes through layers of coarse doormat to dampen the flow, after that it passes through flow straightener to minimize the turbulence of the flow, then it passes through a 50 cm long distance inside the empty enclosure of the damper to ensure that the flow is fully-developed. After the damper, air goes to the transparent section were the laser beams are focused at the point of interest to measure the velocity at that point. As it was mentioned in section 4.2, measurements were taken at 24 points to visualize the flow field. Figures 5.2, 5.3 and 5.4 show the horizontal velocity profiles at heights of 5 cm, 10 cm and 15 cm, respectively, for a flow velocity of 1.0 m/s.

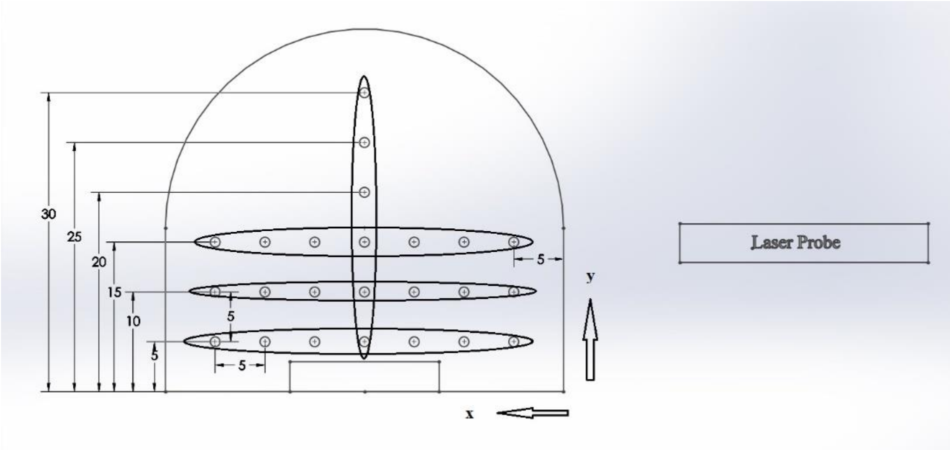

Figure 5.1. Velocity profiles measured using LDA

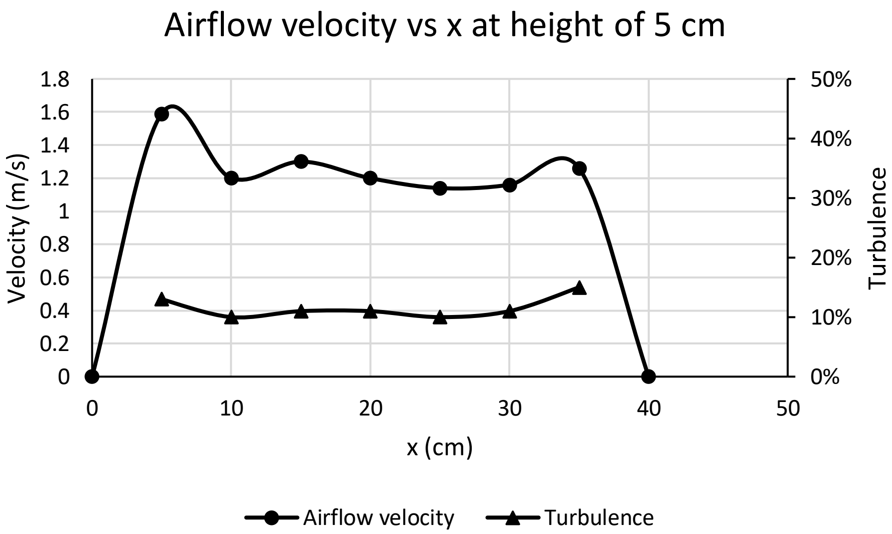

Figure 5.2. Velocity profile and turbulence intensity at height of 5 cm

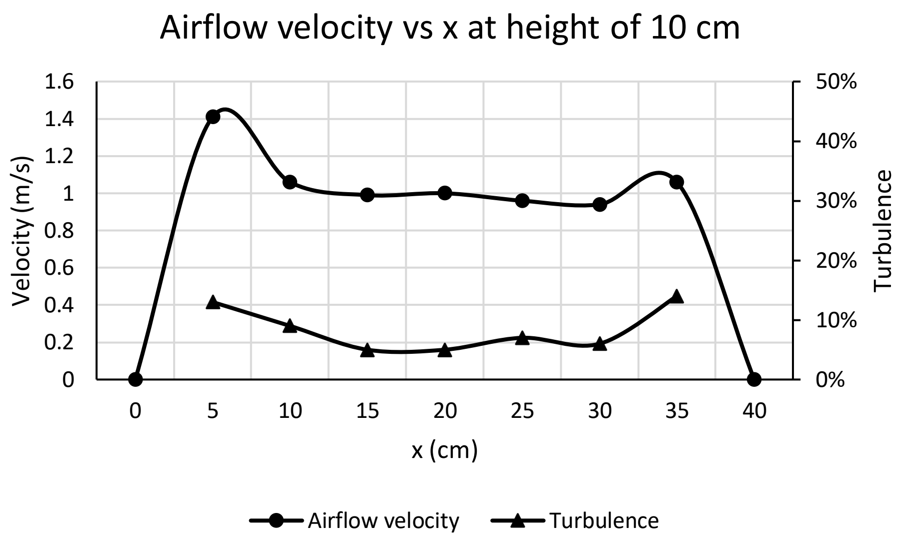

Figure 5.3. Velocity profile and turbulence intensity at height of 10 cm

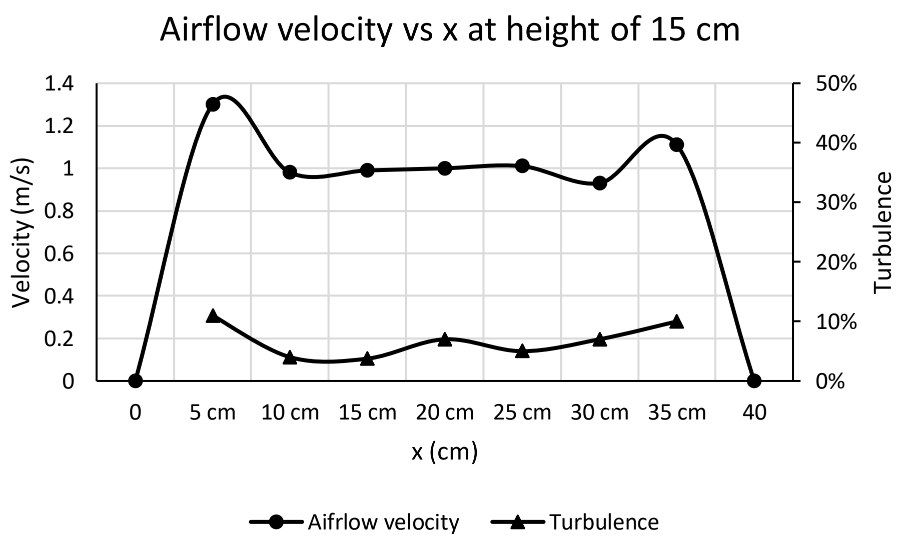

Figure 5.4. Velocity profile and turbulence intensity at height of 15 cm

Graphs above show that velocity is almost constant along the x-axis at all heights except near the walls at x= 5 cm and x= 35 cm; the reason of the slight increase at those points is due to the slight gap between the mat layers and the walls of the damper as the mat layers where cut by hand which resulted in inferior finishing of the edges. Also, the layers where attached to each other by an iron wire, and because the mat is a flexible material, it was difficult to keep the edges of the eight layers fully stretched.

Each layer had some folds on some places along the circumference, Figure 3.17, which indeed made the mesh less dense at all edges. That also explains why velocity is higher, by 0.2 m/s, and more turbulent at a height of 5 cm which is the closest to the walls of the damper. Figure 5.5 shows velocity profile along the centerline of the tunnel. Except for a height of 5 cm, velocity had a maximum value 1.04 m/s at the ceiling and a minimum value of 0.93 m/s at a height of 20 cm where the curvature of the tunnel begins. Tunnel characterization results show that the flow is uniform throughout the tunnel with slight increase near the edges, also turbulence intensity values were between 4% and 15% at all points, which is good for tunnels with blower type fans. Flow characterization was done for 0.5 m/s and 1.5 m/s velocities and similar profiles were obtained at those two velocities. The profiles are given in appendix A.

In the previous studies that has been conducted using the setup [42, 43, 61, 14, 16, 44], velocity was measured using a hotwire anemometer at 5 cm height intervals and then a mean value was taken; However, the previous setup had less flow uniformity compared to the new configuration. The hotwire is shown to read the flow velocity slightly less than the actual value when compared with LDA measurements. This means that the results given in this study are more accurate compared to the ones conducted on the previous setup. Therefore, there can be some discrepancies when comparing the results of two works. In the following sections, results will be investigated to understand the effect of flow uniformity on the HRR, temperature distribution and critical ventilation velocity. Results will also be compared with the experiments from the previous tunnel model [16].

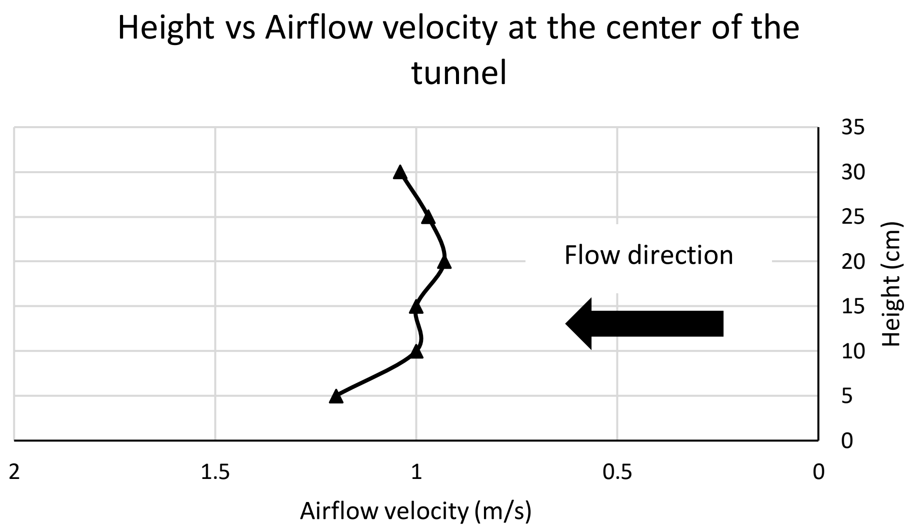

Figure 5.5. Velocity profile the centerline at of the tunnel

5.2. Effect of ventilation on HRR

It was discussed in section 2.4.1 that HRR is considered "*the single most important variable in fire hazard*" [17], so it is of crucial importance to understand the effect of airflow velocity on the HRR. In this section, results of the effect of airflow velocity on HRR are presented and analyzed.

It was mentioned in section 2.4.1 that there are two methods used in literature to calculate the HRR, (i) using the MLR of the fire and (ii) the OCCM. In this work MLR method was used. HRR was calculated according to the following equation assuming 100% combustion efficiency of ethanol as a non-sooting clean fuel [14]

$$\dot{Q} = H_c\left(\frac{dm_{fu}/dt}{A_{Burned}}\right) \quad (5.1)$$

where H_c is the heat of combustion of ethanol of 29.664 MJ/kg. Burning rate calculation was explained in section 3.4.3.

In section 1.2, it was mentioned that in confined spaces, fires exhibit five stages: (1) ignition, (2) fire growth, (3) flashover, (4) fully developed fire and (5) decay and extinction. Figure 5.6 shows the evolution of burning rates at different ventilation velocities. It can be noticed that increasing ventilation velocity enhances the burning rate as it increases the oxygen availability [14, 62]. Results also imply that the steady state combustion stage, or fully developed fire stage, becomes shorter at high velocities for the same amount of fuel; and for high enough velocities like 1.75 m/s, the decay stage starts before the fire is fully developed. In the future, steady state fuel feeding system can be designed and integrated with the setup, in this way it will be possible to reach the fully developed fire stage at higher velocities as well.

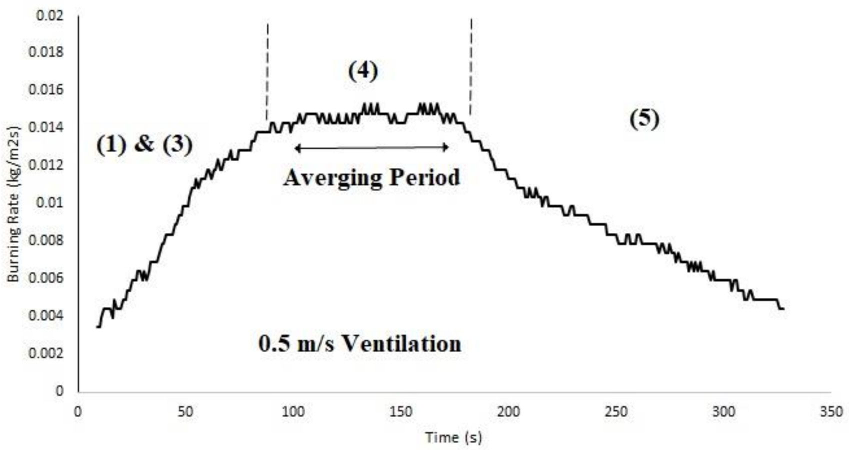

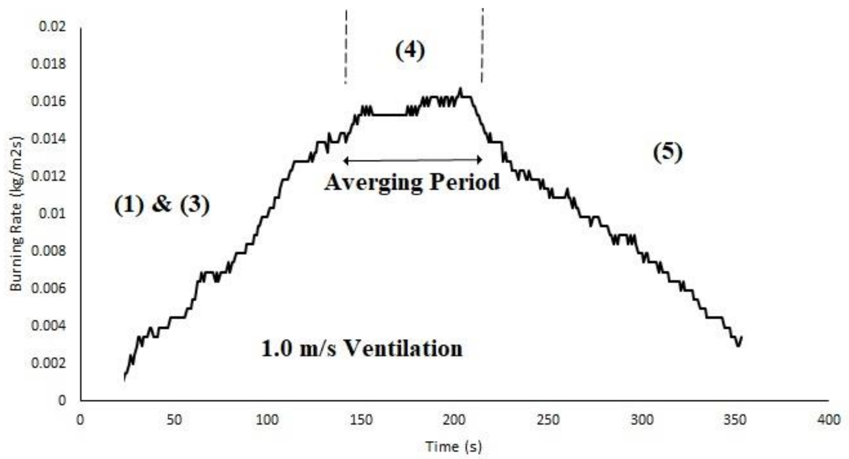

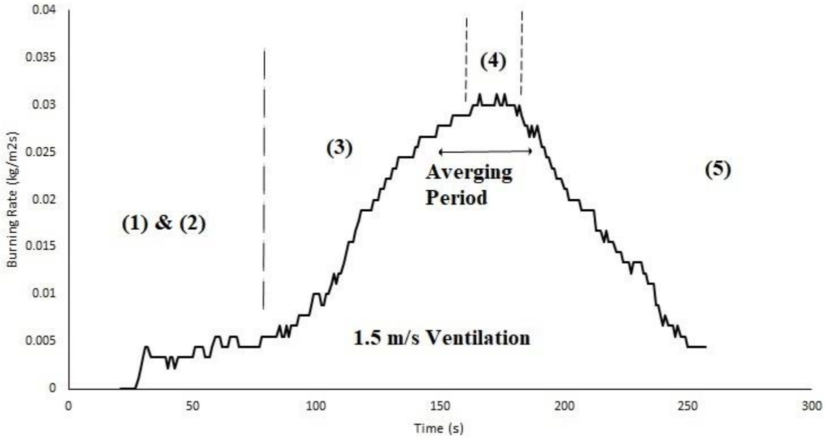

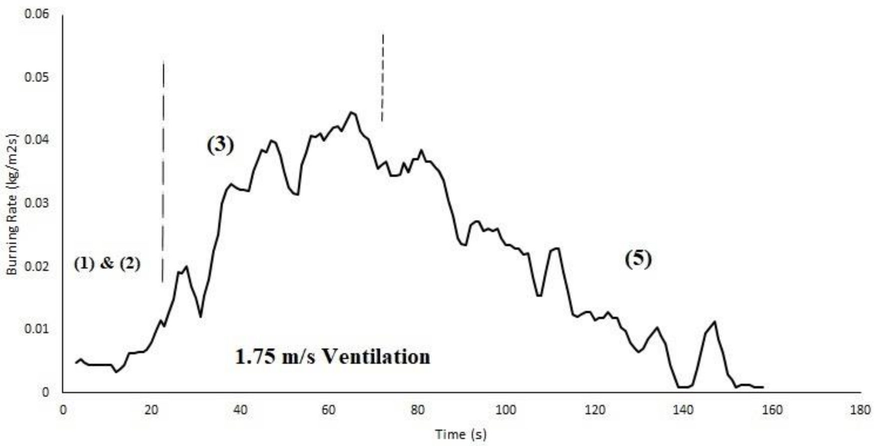

Figure 5.6. Temporal evolution of burning rate at different ventilation velocities

HRR flux at each ventilation velocity was reported as the value corresponding to the time-averaged maximum value of burning rate, which was obtained in the quasi-steady-state combustion period in which burning rate is constant for a period of time. Figure 5.6 shows that at high velocities, like 1.75 m/s, the burning rate results were not stable, that was due to the ineligible fluctuations in the load cell caused by the flame interactions with the airflow. Because of that, cases of ventilation velocities above 1.5 m/s were not studied.

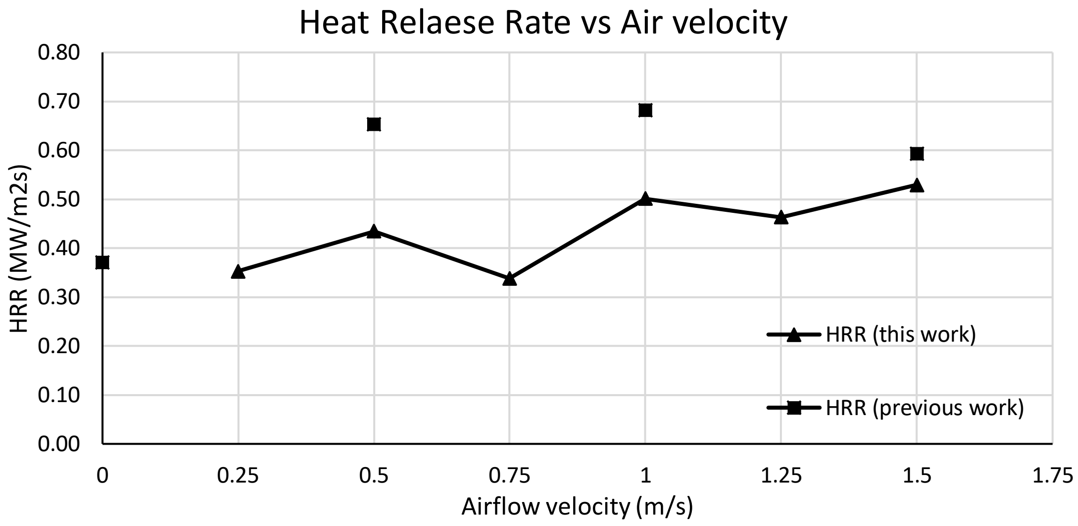

Figure 5.7. HRR vs airflow velocity

Results in Figure 5.7 show that HRR, similar to burning rate, increases as ventilation velocity is increased. When compared to the work of Shafee et al., HRR values of this work were always lower than those in Shafee et al. The discrepancy between the two results varied between 15% and 50%, it can be noticed that this discrepancy decreases as velocity increases. It is not easy to explain the reason for this discrepancy, however, as discussed before, this might be due to the difference in flow uniformity and the different reading in the hotwire anemometer for flow velocity. This indicates that flow uniformity has significant effect on the HRR; less uniformity result in higher HRR values.

5.3. Effect of ventilation on temperature distribution

The maximum gas temperature beneath the ceiling is considered one of the most important parameters in designing fireproofing materials for tunnels. High temperature values, above 300 °C, at the ceiling may cause damage to the steel reinforcement of the tunnel lining concrete [63]. Figure 5.8 shows the maximum temperature distribution along the ceiling at different ventilation velocities. Results show that the maximum gas temperature is reached above the fuel tray for low velocities, while the location of the maximum gas temperature shifts to the downstream as the airflow velocity is increased. Recalling that critical ventilation velocity is the minimum ventilation velocity needed to push all the smoke downstream of the tunnel, Figure 5.8 shows that the critical ventilation velocity lies between 0.75 m/s and 1.0 m/s. This led to conducting two more experiments at 0.8 m/s and 0.85 m/s to know the exact critical velocity, more details in section 5.4. Results also show that increasing ventilation velocity leads to lower maximum ceiling temperature values in the downstream when the ventilation velocity is below the critical velocity, while further increase in the ventilation velocity for magnitudes above the critical velocity results in increasing the maximum ceiling temperature.

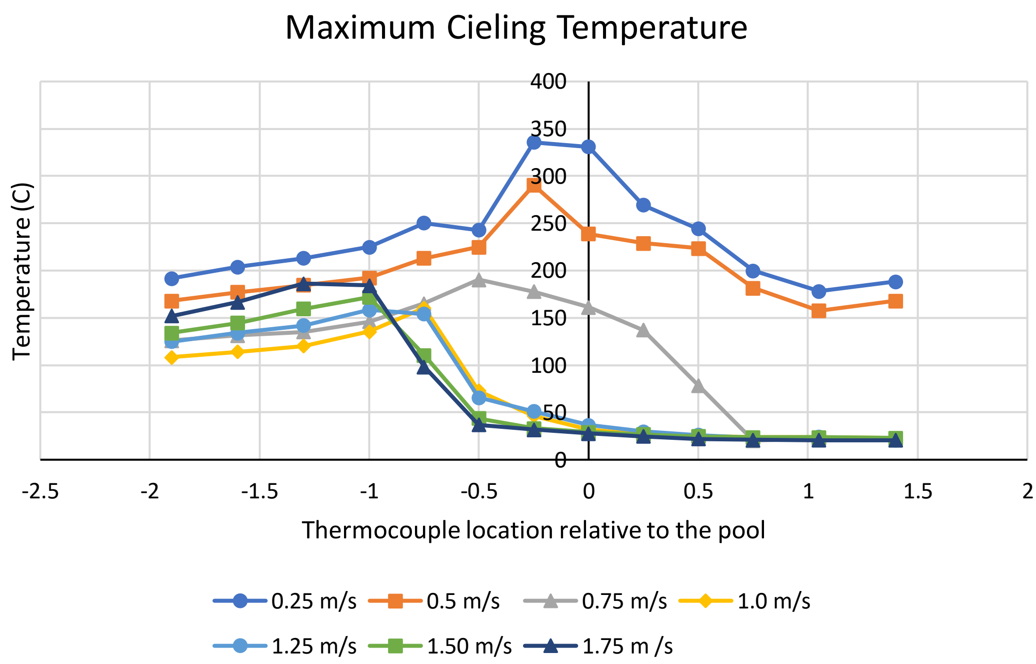

Figure 5.8. Maximum ceiling temperature along the tunnel at different ventilation velocities

5.4. The critical ventilation velocity

The critical ventilation velocity in this work was determined by analyzing the maximum ceiling temperature profiles at different velocities, and the minimum velocity for which there was no temperature increase from the incoming is the critical ventilation velocity. Figure 5.9 shows the maximum ceiling temperature profiles for velocities of 0.75 m/s, 0.80 m/s, 0.85 m/s and 1.0 m/s. It can be noticed that there is temperature increase in the upstream for 0.75 m/s and 0.80 m/s, but this is not the case for 0.85 m/s and 1.0 m/s. As a result, the critical ventilation velocity was found to be between 0.80 m/s and 0.85 m/s for this tunnel model, this critical ventilation value corresponds to a value around 3 m/s in full-scale tunnel.

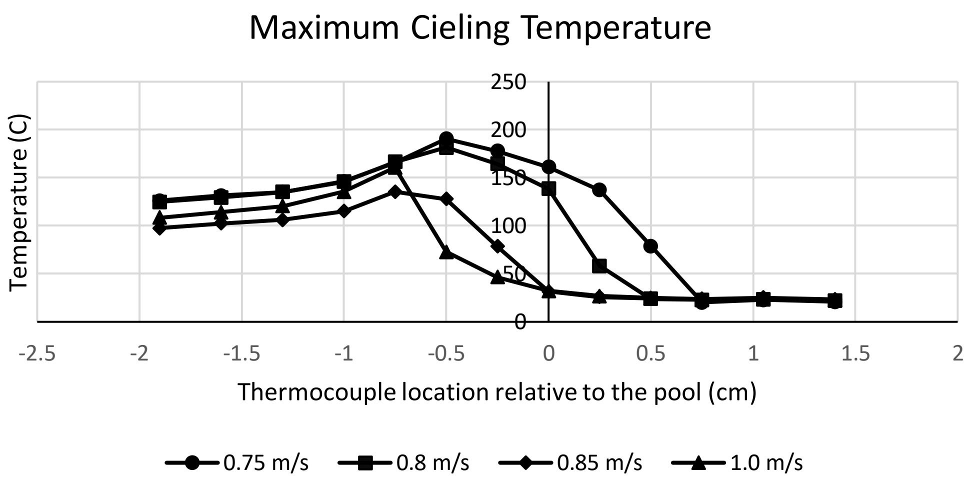

Figure 5.9. Maximum ceiling temperature along the tunnel at different ventilation velocities

In section 2.4.2 five models for calculating the critical ventilation velocity in tunnels were discussed. The most commonly used model is the one adopted by NFPA based on the critical Froude number model discussed in section 2.4.2.1 [5]. Figure 5.10 compares the critical ventilation velocity calculated in this work to the predicted results by the models in the literature. It can be noticed that generally speaking all models under-predicted the critical velocity. This can be due to several effects including assumption of uniformity in the ventilating air in those models. It can also be seen that the estimated critical velocity was higher in previous work using the model, which can be because of the higher turbulence in the ventilation flow used in that work.

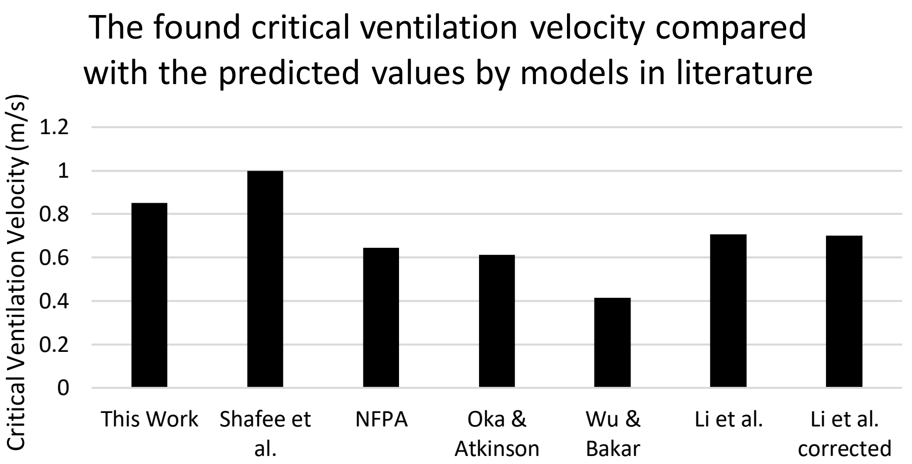

Figure 5.10. The critical ventilation velocity compared to other models available in literature [44, 5, 34, 35, 36, 37]

5.5. Effect of combustion on velocity profile in the upstream

In this section, the backlayering thickness at the upstream of fire is studied. All experiments for ventilation velocity between 0.35 m/s and 1.75 m/s were conducted at least three times. At each time, velocity history was recorded at one of the three points on the center-line of the tunnel in the upstream using LDA for 30 seconds time interval. For velocities between 0.55 m/s and 1.75 m/s LDA measurements were taken at heights of 5 cm, 15 cm and 25 cm respectively, but the LDA readings remained constant during the whole combustion process. This is because backlayering length was shorter than 2.5 m which is the place at which the LDA measurements were taken. Variation in the LDA readings started at ventilation velocity of 0.5 m/s. It was noticed that velocity is increasing at heights of 5 cm and 15 cm as combustion is taking place, but when the laser beams were traversed to a height of 25 cm, the LDA didn't give valid readings. So, the beams were traversed down until valid readings were achieved at a height of 23.5 cm. This implies that the thickness of the backlayering is 11.5 cm, and any attempt to measure the velocity at heights above 23.5 cm will not give valid results using LDA since it will be within the backlayering of the smoke where the smoke of the fire is moving in the upstream with high turbulence. So, instead of recording the LDA readings at a height of 20 cm, it was recorded at a height of 20 cm. Figure 5.11 shows the backlayering thickness at the LDA measurement location for different ventilation velocities. For ventilation velocities of 0.4 m/s and 0.35 m/s, the backlayering thickness is higher than 15 cm, which means that readings cannot be taken at a height of 20 cm, so velocity was recorded at heights of 5 cm and 15 cm only.

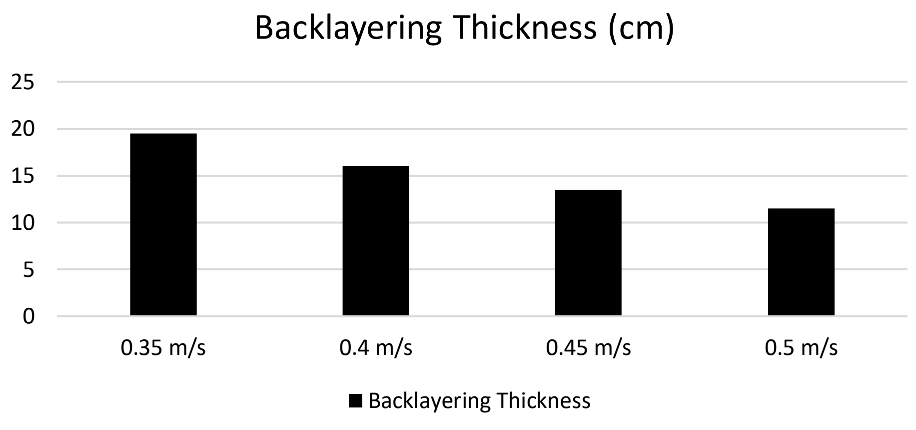

Figure 5.11. Backlayering thickness for different ventilation velocities

Figure 5.12 shows the velocity history recorded at a height of 5 cm for ventilation velocity of 0.5 m/s. It can be noticed that velocity increases up 0.71 m/s when combustion takes place and then it starts to decrease again to the initial velocity when the fire reaches the decay stage. This increase is because the backlayering has blocking effect on the airflow coming from the fan, the backlayering decreases the effective area from which the airflow passes, but as the air mass flow rate supplied by the fan is constant, the airflow velocity increases to compensate the decrease of the effective area resulting from the formation of the backlayering. To express the increase of the airflow velocity below the backlayering, a new non-dimensional number is presented called the ‘non-dimensional ventilation velocity’ which is defined as the airflow ventilation velocity when the combustion is taking place per the ventilation velocity in the cold flow.

$$V^* = \frac{V_{avg,hot}}{V_{cold}} \tag{5.2}$$

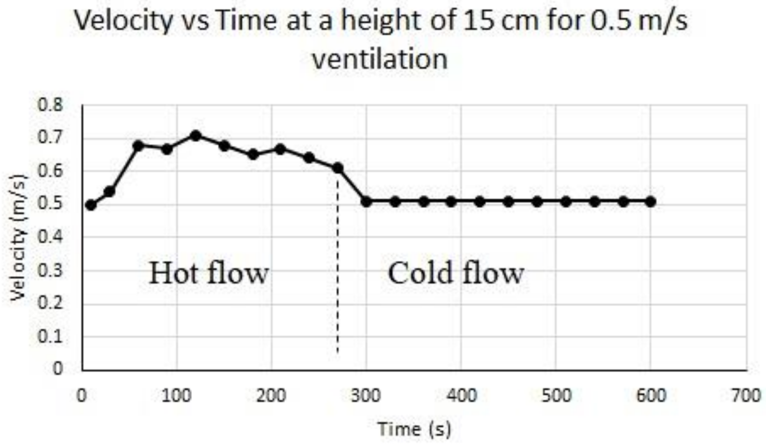

Figure 5.12. Velocity history at a height of 15 cm for 0.5 m/s ventilation

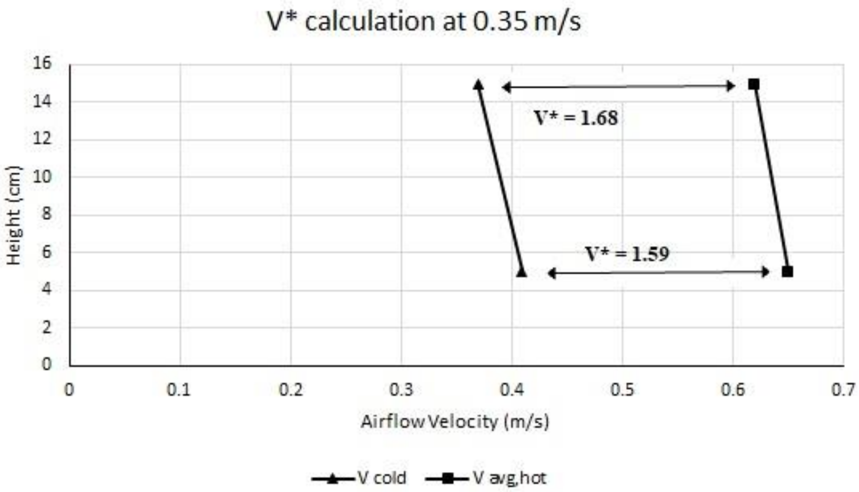

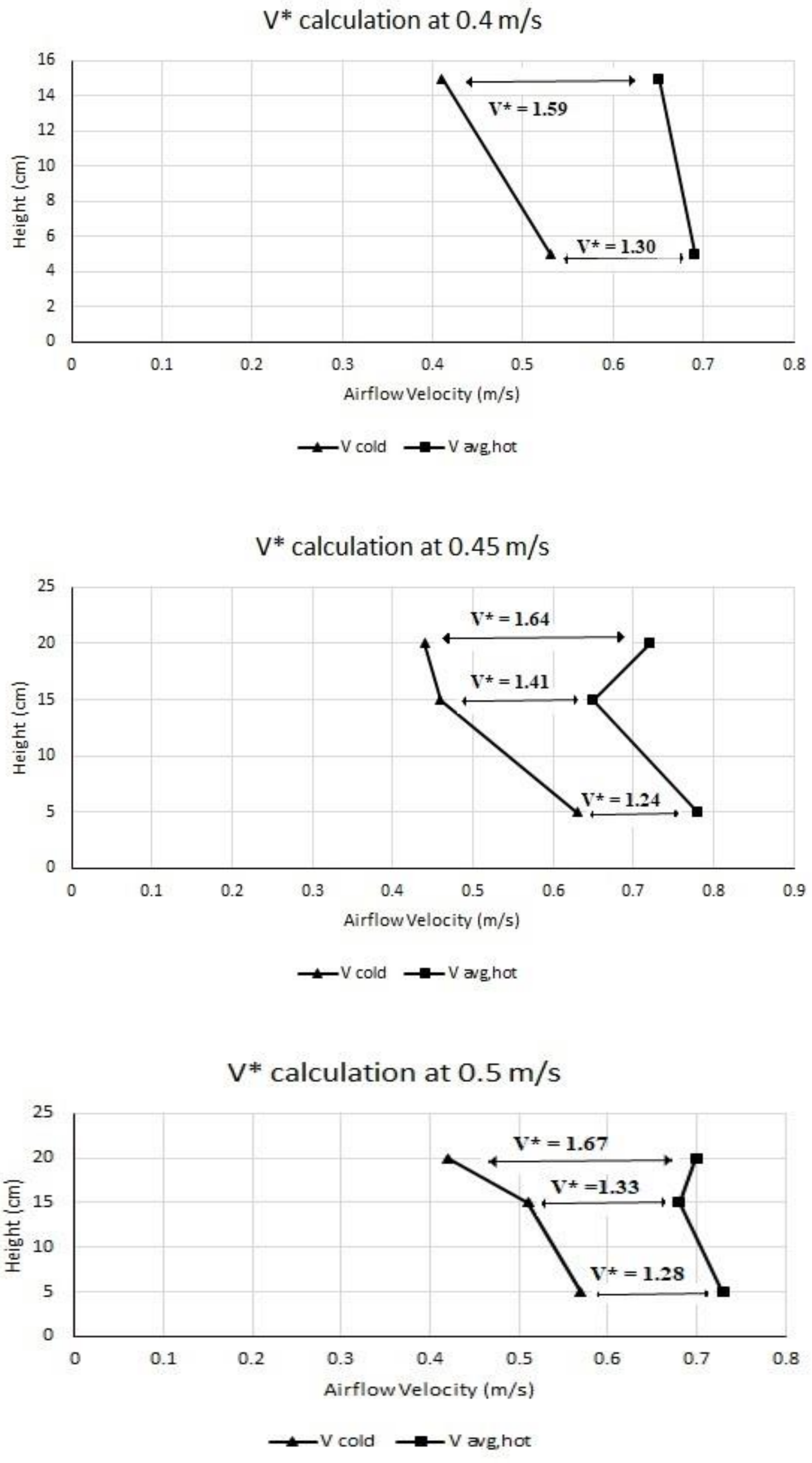

Figure 5.13. Non-dimensional velocity for (a) 0.35 m/s (b) 0.40 m/s (c) 0.45 m/s and (d) 0.50 m/s

Figure 5.13 shows that for all cases velocity increases more, has higher V* values, when the point of measurement is closer to the ceiling. The average V* is calculated and presented in Figure 5.14. It was previously shown that lower velocities result in thicker backlayering, by looking at Figure 5.14 it is shown that lower velocities has higher non-dimensional velocities, which means that the backlayering has blockage effect that decreases the effective area for ventilation flow. Minimum blockage was observed at ventilation velocity of 0.5 m/s with 43% increase in velocity below the backlayering. The blocking effect increases as the velocity drops reaching 63% velocity increase at ventilation velocity of 0.35 m/s. In the future, Particle Image Velocimetry (PIV) will be integrated in the setup to have a full velocity profile across the tunnel which will result in more detailed visualization of the profile including the sides of the tunnel.

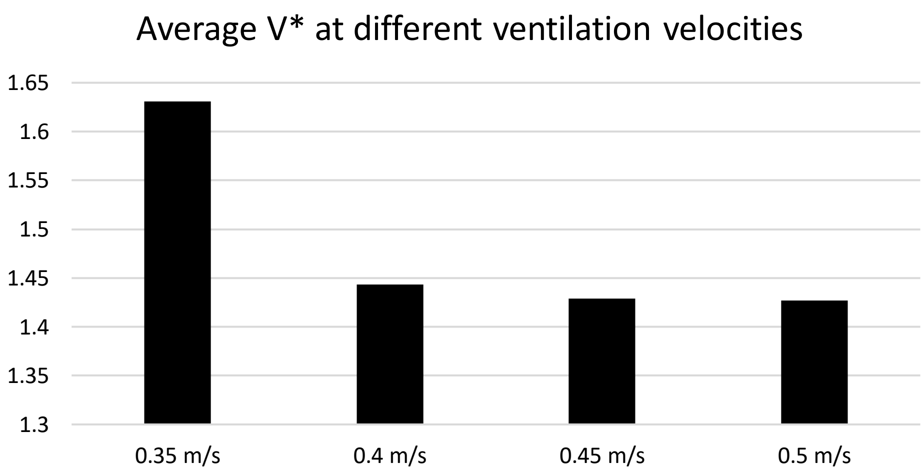

Figure 5.14. Average V* at different ventilation velocities

CHAPTER 6

CONCLUSIVE REMARKS

Tunnel fires remain a major threaten to the lives of passengers and motorists. Designing tunnel fire safety systems need good understanding of fire burning characteristics in confined spaces. The purpose of this study was to renovate a 1/13 tunnel model used in studying pool fires in confined spaces to have better means of control and accuracy of the experiments to acquire more accurate results. The model was relocated to have more controlled environment in order to eliminate the effect of the surroundings. The main parts of the model were renewed, and new and more controllable equipment was added. In the second stage of this research, tunnel flow characterization was conducted using LDA method both in hot and cold flow cases to have an idea about the effect of fire on velocity profile of the ventilating air. Finally, experiments were conducted to investigate the effect of airflow velocity on HRR and temperature distribution and to find the critical ventilation velocity of the tunnel. In the hot flow experiments, 100 ml of ethanol were burned in a 15 cm square fuel tray. Temperature values were recorded throughout the tunnel and mass history of the fuel was recorded to calculate the burning rate of the fuel. The following conclusions can be drawn from the experimental results:

- Results show that HRR, burning rate and temperature distribution is significantly affected by the ventilating air.
- HRR increases by increasing the airflow velocity
- There is no temperature increase at ventilation velocity of 0.85 m/s, so the critical ventilation velocity is found to be between 0.80 m/s and 0.85 m/s.
- By comparing the results found in this work with the results of other works conducted on the same setup before renovation, it is found that HRR, burning

rate, temperature distribution and the critical ventilation velocity are affected by flow uniformity.

- Higher temperature values, up to 300 °C, were noticed at low ventilation velocities which might damage the tunnel coating and lining materials.
- Results imply that the critical ventilation velocity is higher in tunnels with more turbulent airflows.
- Results show that the backlayering length and thickness increase when the ventilation velocity is increased below the critical ventilation velocity.
- It was shown that the backlayering decreases the effective area of the incoming flow which causes the velocity of the airflow to increase beneath the backlayering.
- A new non-dimensional number, the non-dimensional velocity, was introduced to represent the fractional velocity increase in the upstream for ventilation velocities lower than the critical ventilation velocity.
- It was shown that the non-dimensional velocity is maximum near the backlayering and it decreases gradually until a minimum value is obtained at the bottom of the tunnel.
- It was shown that the average non-dimensional velocity is higher for lower ventilation velocities.

REFERENCES

[1] Moorey, Peter Roger Stuart (1999) [1994]. Ancient Mesopotamian Materials and Industries: The Archaeological Evidence. Winona Lake, Indiana: Eisenbrauns.

[2] Spartacus Educational. (2018). Transport and the Industrial Revolution. [online] Available at: https://spartacus-educational.com/U3Ahistory17.htm [Accessed 5 Nov. 2018].

[3] Walton WD, Thomas PH, Ohmiya Y. Estimating Temperatures in Compartment Fires. SFPE Handb. Fire Prot. Eng., New York, NY: Springer New York; 2016, p. 996–1023. doi:10.1007/978-1-4939-2565-0_30.

[4] Beard, A., & Carvel R. The handbook of tunnel fire safety. London: Thomas Telford; 2005.

[5] National Fire Protection Association, 2011. NFPA 502: Standard for Road Tunnels, Bridges, and Other Limited Access Highways, 2011 Edition.

[6] 2011 ASHRAE handbook. (2011). Atlanta, Ga.: ASHRAE.

[7] Lotsberg.net. (2018). Railroad and Metro Tunnel Accidents. [online] Available at: http://www.lotsberg.net/artiklar/andersen/en_table_1.html [Accessed 5 Nov. 2018].

[8] Carvel, R., and Marlair, G, "A History of Fire Incidents in Tunnels," The Handbook of Tunnel Fire Safety, ed. Beard, A., and Carvel, R., pub. Thomas Telford, London, 2005, pp. 3-37.

[9] AIPCR, 1999. Fire and Smoke Control in Road Tunnels, Association Internationale Permanente des Congrès de la route, http://www.piarc.org.

[10] Chiefscientist.nsw.gov.au. (2018). [online] Available at: http://www.chiefscientist.nsw.gov.au/__data/assets/pdf_file/0009/54792/Road-Tunnels_TP04_Road-Tunnel-Ventilation-Systems.pdf [Accessed 3 Jul. 2018].

[11] Li, J. and Chow, W. (2003). Numerical studies on performance evaluation of tunnel ventilation safety systems. Tunnelling and Underground Space Technology, 18(5), pp.435-452.

[12] Carvel, R., Beard, A., Jowitt, P. and Drysdale, D. (2001). Variation of heat release rate with forced longitudinal ventilation for vehicle fires in tunnels. Fire Safety Journal, 36(6), pp.569-596.

[13] Quintiere, J. (2008). Fundamentals of fire phenomena. Chichester: Wiley.

[14] Shafee, S. and Yozgatligil, A. (2018). An experimental study on the burning rates of interacting fires in tunnels. Fire Safety Journal, 96, pp.115-123.

[15] Yi L, Xu Q, Xu Z, Wu D. An experimental study on critical velocity in sloping tunnel with longitudinal ventilation under fire. Tunn Undergr Sp Technol 2014;43:198–203. doi:10.1016/j.tust.2014.05.017.

[16] Shafee, S 2017, An experimental and numerical study on the combustion characteristics of pool fires in tunnels ', Ph.D thesis, Middle East Technical University, Ankara, Turkey.

[17] Babrauskas, V. and Peacock, R. (1992). Heat release rate: The single most important variable in fire hazard. Fire Safety Journal, 18(3), pp.255-272.

[18] B. Chen, S.X. Lu, C.H. Li, Q.S. Kang, V. Lecoustre, Initial fuel temperature effects on burning rate of pool fire, J. Hazard Mater. 188 (2011) 369–374, https://doi.org/10.1016/j.jhazmat.2011.01.122.

[19] Chow, W. and Han, S. (2011). Heat release rate calculation in oxygen consumption calorimetry. Applied Thermal Engineering, 31(2-3), pp.304-310.

[20] Huggett, C. (1980). Estimation of rate of heat release by means of oxygen consumption measurements. Fire and Materials, 4(2), pp.61-65.

[21] Heat Release Rates for Materials and Products Using an Oxygen Consumption Calorimeter, (revision and redesignation of ANSI/NFPA 264-1995), ANSI/NFPA 271-1998, National Fire Protec-tion Association, Quincy, MA (1998).

[22] Parker, W. (1982). Calculations of the heat release rate by oxygen consumption for various applications. Washington, DC: U.S. Dept. of Commerce, National Bureau of Standards.

[23] Chen, C., Xiao, H., Wang, N., Shi, C., Zhu, C. and Liu, X. (2017). Experimental investigation of pool fire behavior to different tunnel-end ventilation opening areas by sealing. Tunnelling and Underground Space Technology, 63, pp.106-117.

[24] S. Brohez, C. Delvosalle, G. Marlair, A. Tewarson, Soot generation in fires: an important parameter for accurate calculation of heat release, in: Fire Safety Science Proceedings of the Sixth International Symposium, 1999, pp.265 e276.

[25] Hamins A, Johnsson E, Donnelly M, Maranghides A. Energy balance in a large compartment fire. Fire Saf J 2008;43:180–8. doi:10.1016/j.firesaf.2007.08.002.

[26] Bryant R, Mulholland G. A guide to characterizing heat release rate measurement uncertainty for full-scale fire tests. Fire Mater 2008:121–39. doi:10.1002/fam.

[27] Pretrel, H., Le Saux, W. and Audouin, L. (2013). Determination of the heat release rate of large-scale hydrocarbon pool fires in ventilated compartments. Fire Safety Journal, 62, pp.192-205.

[28] Janssens ML. Measuring rate of heat release by oxygen consumption. Fire Technol 1991;27:234–49. doi:10.1007/BF01038449.

[29] Sensenig DL, States. U, (U.S.) C for FR. An oxygen consumption technique for determining the contribution of interior wall finishes to room fires 1980:86 in various pagings.

[30] P.H. Thomas, The Movement of Buoyant Fluid against a Stream and the Venting of Underground Fires, Fire Research Station, Fire Research Notes 351, Borehamwood, 1958, p. 9.

[31] P.H. Thomas, The Movement of Smoke in Horizontal Passages Against an Air Flow, Fire Research Station, Fire Research Notes 723, Borehamwood, 1968, p. 9.

[32] N.H. Danziger, W.D. Kennedy, Longitudinal Ventilation Analysis for the Glenwood Canyon Tunnels, in: Proceedings of the Fourth International Symposium on the Aerodynamics & Ventilation of Vehicle Tunnels, BHRA Fluid Engineering, York, UK, 1982, pp. 169 – 186.

[33] W.D. Kennedy, Critical velocity: Past, Present and Future, Seminar of Smoke and Critical Velocity in Tunnels, JFL Lowndes, London, 1996, pp. 305 – 322.

[34] Y. Oka, G.T. Atkinson, Control of smoke flow in tunnel fires, Fire Saf. J. 25 (1995)305–322. http://dx.doi.org/10.1016/0379-7112(96)00007-0.

[35] Wu, M.Z.A. Bakar, Control of smoke flow in tunnel fires using longitudinal ventilation systems-a study of the critical velocity, Fire Saf. J. 35 (2000) 363–390. http://dx.doi.org/10.1016/S0379-7112(00)00031-X.

[36] Y.Z. Li, B. Lei, H. Ingason, Study of critical velocity and backlayering length in longitudinally ventilated tunnel fires, Fire Saf. J. 45 (2010) 361–370. http://dx.doi.org/10.1016/j.firesaf.2010.07.003.

[37] Li, Y. and Ingason, H. (2017). Effect of cross section on critical velocity in longitudinally ventilated tunnel fires. Fire Safety Journal, 91, pp.303-311.

[38] Batchelor, G. (2000). Introduction to Fluid Mechanics.

[39] BSA Flow Software Version 4.10 Installation & User's Guide. (2016). Skovlunde: Dantec Dynamics.

[40] Ingason H. State of the Art of Tunnel Fire Research. Fire Saf Sci 2008;9:33–48. doi:10.3801/IAFSS.FSS.9-33.

[41] Bechtel P. Memorial Tunnel Fire Ventilation Test Program Test Report. 1995.

[42] Kayili, S., Yozgatligil, A. and Cahit Eralp, O. (2011). An experimental study on the effects of blockage ratio and ventilation velocity on the heat release rate of tunnel fires. Journal of Fire Sciences, 29(6), pp.555-575.

[43] Kayili, S., Yozgatligil, A. and Eralp, O. (2012). Effect of Ventilation and Geometrical Parameters of the Burning Object on the Heat Release Rate in Tunnel Fires. Combustion Science and Technology, 184(2), pp.165-177.

[44] Shafee, S. and Yozgatligil, A. (2018). An analysis of tunnel fire characteristics under the effects of vehicular blockage and tunnel inclination. Tunnelling and Underground Space Technology, 79, pp.274-285.

[45] YEH Y. and CUMMINS H.Z. Localized Fluid Flow measurements with an He-Ne Laser Spectrometer Applied Physics Letters 15 May 1964.

[46] Dantec Dynamics, "Laser Optical Measurement Systems and Sensors", http://www.dantecdynamics.com/laser-doppler-anemometry, July 2013.

[47] Tropea, C. (1995). Laser Doppler anemometry: recent developments and future challenges. Measurement Science and Technology, 6(6), pp.605-619.

[48] Durst, F., A. Melling, and J. Whitelaw. 1981. Principles and Practices of Laser-Doppler Anemometry. Academic Press.

[49] Thermocoupleinfo.com. (2018). Type K Thermocouple. [online] Available at: https://www.thermocoupleinfo.com/type-k-thermocouple.htm [Accessed 5 Nov. 2018].

[50] Hansen, R. (2018). Fire behaviour of multiple fires in a mine drift with longitudinal ventilation. International Journal of Mining Science and Technology.

[51] He, Q., Ezekoye, O., Li, C. and Lu, S. (2015). Ventilation limited extinction of fires in ceiling vented compartments. International Journal of Heat and Mass Transfer, 91, pp.570-583.

[52] Zhou, L., Zeng, D., Li, D. and Chaos, M. (2017). Total radiative heat loss and radiation distribution of liquid pool fire flames. Fire Safety Journal, 89, pp.16-21.

[53] Yi, L., Xu, Q., Xu, Z. and Wu, D. (2014). An experimental study on critical velocity in sloping tunnel with longitudinal ventilation under fire. Tunneling and Underground Space Technology, 43, pp.198-203.

[54] Ji, J., Wan, H., Gao, Z., Fu, Y., Sun, J., Zhang, Y., Li, K. and Hostikka, S. (2016). Experimental study on flame merging behaviors from two pool fires along the longitudinal centerline of model tunnel with natural ventilation. Combustion and Flame, 173, pp.307-318.

[55] Chen, C., Xiao, H., Wang, N., Shi, C., Zhu, C. and Liu, X. (2017). Experimental investigation of pool fire behavior to different tunnel-end ventilation opening areas by sealing. Tunnelling and Underground Space Technology, 63, pp.106-117.

[56] Roh JS, Ryou HS, Kim DH, Jung WS, Jang YJ. Critical velocity and burning rate in pool fire during longitudinal ventilation. Tunn Undergr Sp Technol 2007;22:262–71. doi:10.1016/j.tust.2006.08.003.

[57] Steinhaus T, Welch S, Carvel R, Torero J. Large-scale pool fires. Therm Sci 2007;11:101–18. doi:10.2298/TSCI0702101S.

[58] Wang, J., Yuan, J., Fang, Z., Tang, Z., Qian, P. and Ye, J. (2018). A model for predicting smoke back-layering length in tunnel fires with the combination of longitudinal ventilation and point extraction ventilation in the roof. Tunnelling and Underground Space Technology, 80, pp.16-25.

[59] Zhao, S., Liu, F., Wang, F. and Weng, M. (2018). Experimental studies on fire-induced temperature distribution below ceiling in a longitudinal ventilated metro tunnel. Tunnelling and Underground Space Technology, 72, pp.281-293.

[60] Kashef, A., Yuan, Z. and Lei, B. (2013). Ceiling temperature distribution and smoke diffusion in tunnel fires with natural ventilation. Fire Safety Journal, 62, pp.249-255.

[61] Shafee, S., Yamali, U. and Yozgatligil, A. (2017). Experimental Investigation on the Mass Loss Rates of Thin-Layered n-Heptane Pool Fires in Longitudinally Ventilated Reduced Scale Tunnel. Combustion Science and Technology, 189(11), pp.1907-1923.

[62] Stahlanwendung S. Fires in Transport Tunnels: Report on Full-scale Tests ; Eureka-Project EU 499: FIRETUN ; Conducted by the Following 9 European Countries: Austria, Finland, France, Germany, Great Britain, Italy, Norway, Sweden, Switzerland. 1995.

APPENDICES

A. Flow Characterization Results for 0.5 m/s and 1.5 m/s Airflow Velocity

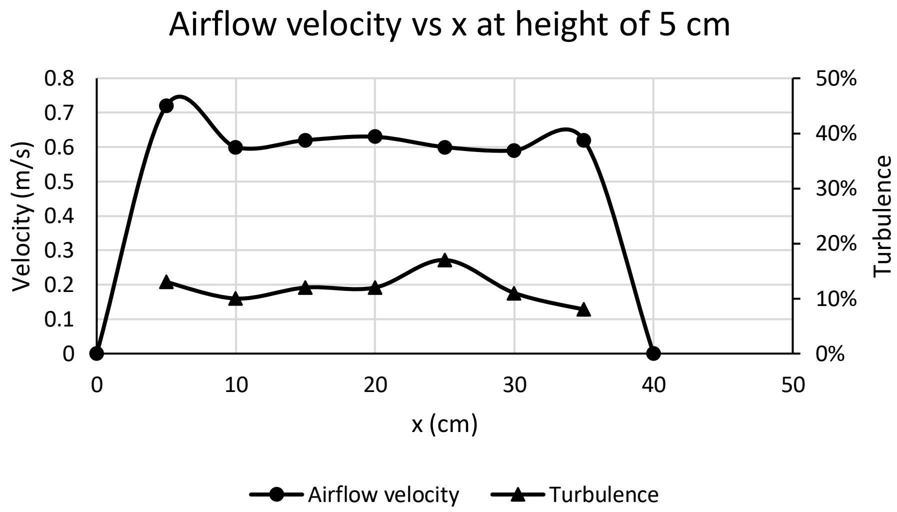

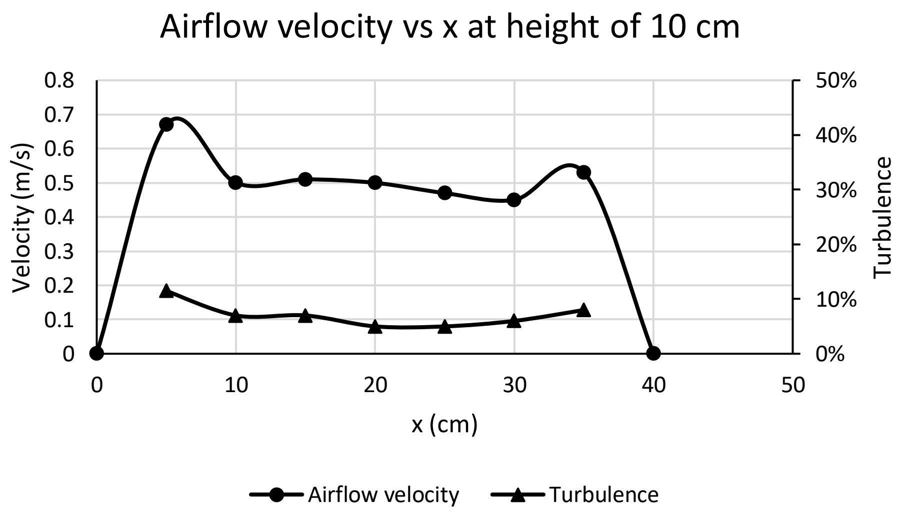

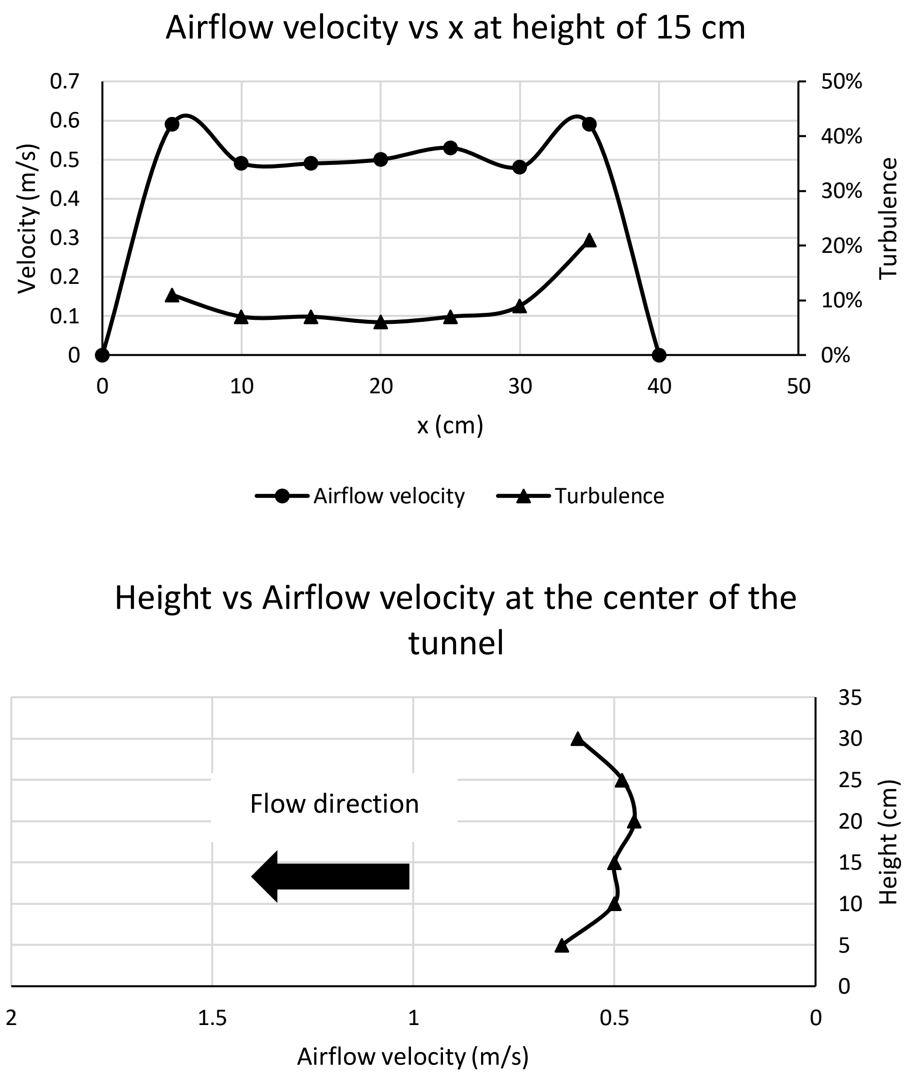

Figure A.1. Flow characterization results at 0.5 m/s ventilation velocity

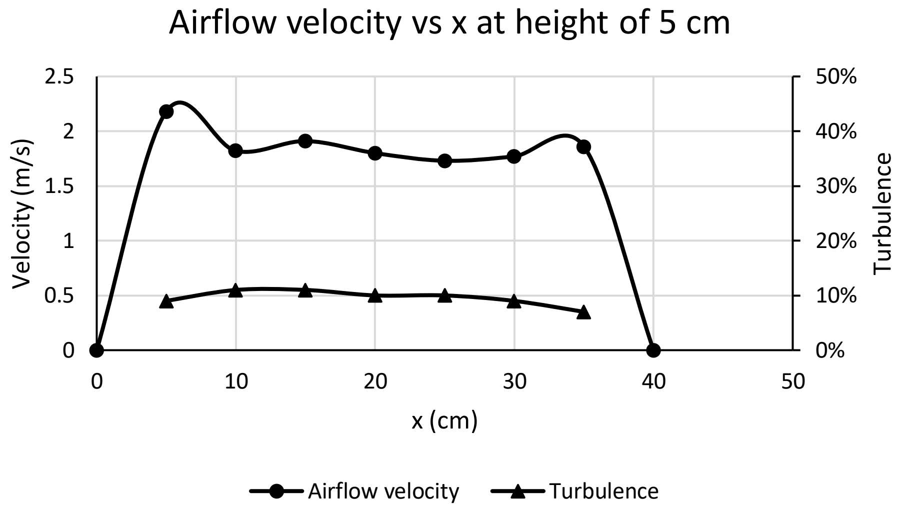

Airflow velocity vs x at height of 5 cm
Velocity (m/s)
Turbulence
x (cm)
Airflow velocity
Turbulence

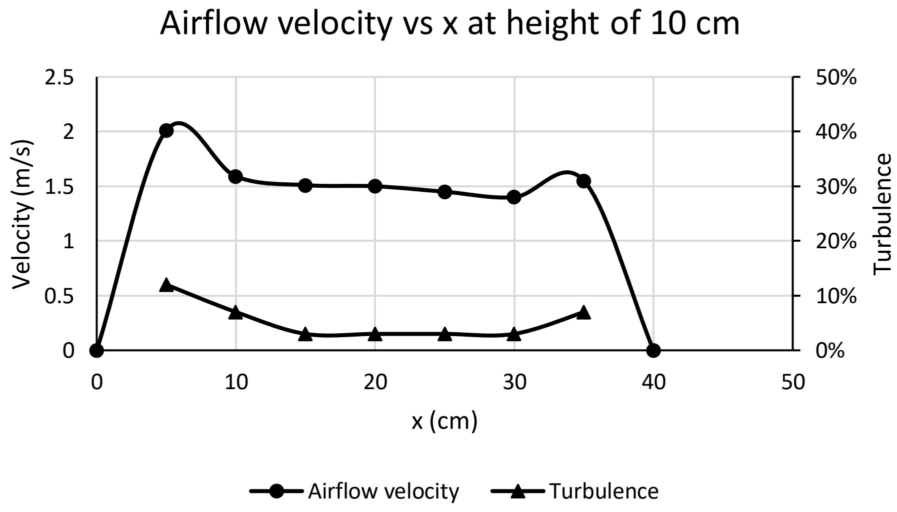

Airflow velocity vs x at height of 10 cm
Velocity (m/s)
Turbulence
x (cm)
Airflow velocity
Turbulence

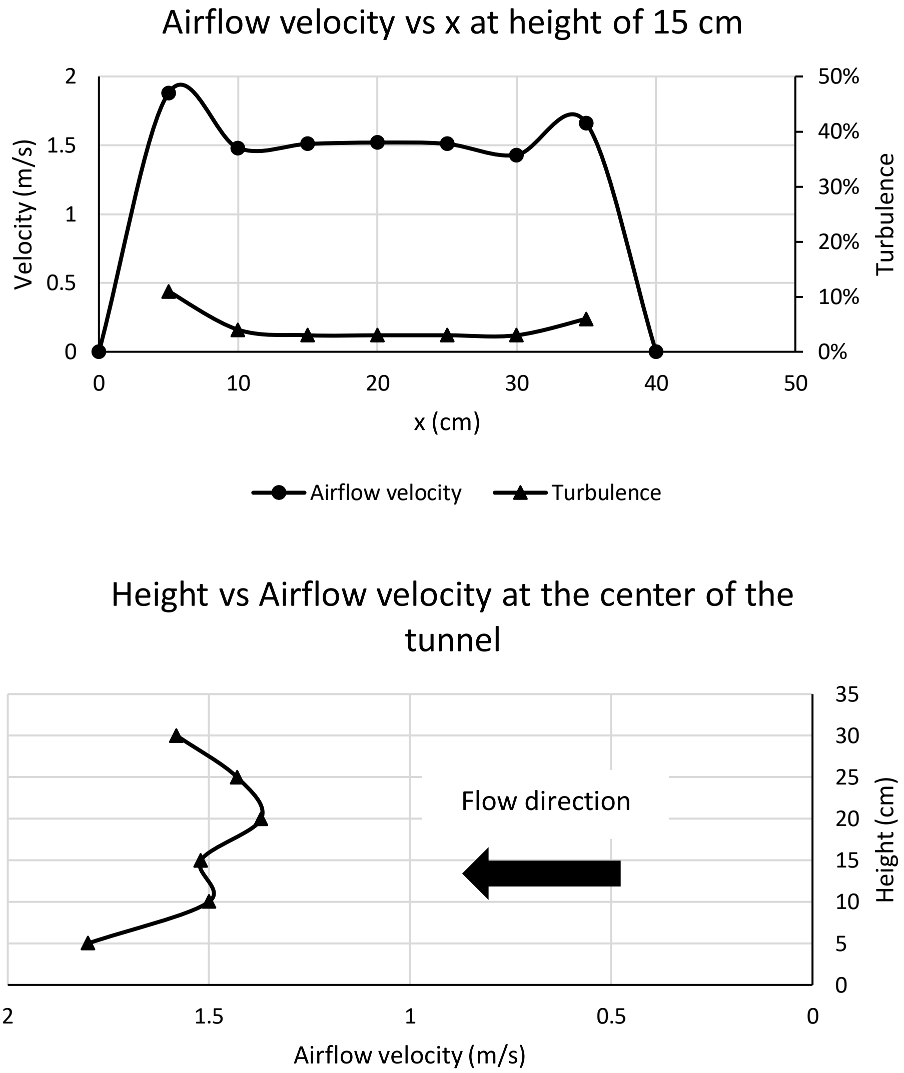

Figure A.2. Flow characterization results at 1.5 m/s ventilation velocity

B. User Guide

The following instructions aim to help the researchers who use the experimental setup to conduct the experiments in the right way to avoid any mistakes that might lead to inaccurate results:

- The fog generator should be at least 1 m away from the fan and the smoke should not be directed at the center of the fan, otherwise the tunnel will be over fed with the tracing particles which leads to high turbulent intensity and low validation values of the results.
- Laser intensity should be high enough to obtain good validation values. Low laser intensity gives low data acquisition rate, while very high intensity may increase the noise of the LDA readings.
- The LDA probe should be aligned parallel to the transparent section to obtain valid results.
- The validation of all the LDA readings should be above 80% to assure good accuracy of the results.
- Before starting the experiments, the fan should be running at full speed for at least 5 minutes to have uniform temperature distribution inside the tunnel with values similar to the temperature inside the lab.
- The load cell should not have any inclination, the water balance on the load shows if the load cell has any inclination.
- The fuel tray should be carefully placed on top of the load cell, the user should assure that there is no contact between the legs of the tray and the metal sheet at the bottom of the combustion zone, otherwise the readings of the load cell will be fluctuating. The user must keep adjusting the load cell's position until the load cell shows a constant and stable reading.
- The airflow exerts a force on the fuel tray, so before pouring the fuel, the fan should be adjusted to the speed of interest, then the tare button on the load cell should be pressed. The same procedure should be repeated whenever the speed of the fan is changed.
- Mass and temperature recording should be started before pouring the fuel

- The required amount of fuel should be poured in a flask. Fuels such as ethanol, n-heptane and diesel are volatile fuels, so the bottle should be closed immediately after pouring the fuel in the flask.
- When the combustion zone is opened, some of the ventilating air will go out through the opening, so the force exerted on the tray by the ventilating air will go down which will result in minus values of the recorded mass readings. The user should the fuel that is in the flask in the fuel tray and close the combustion zone immediately. The readings before closing the combustion zone should be dismissed from the final results.
- Before starting the experiments, a warm up test should be conducted at low ventilation velocity, around 0.5 m/s, to assure uniform temperature distribution inside the tunnel.
- The load cell recording should be stopped as soon as the fire extents at which the load cell reading shows zero value.
- Temperature recording should continue until tunnel completely cools down. All thermocouples should be reading values below 50 °C before starting the new experiment. Increasing the fan speed makes the cooling process faster.
- To study the velocity profile change during the hot flow experiments, the laser should be pointing at the point of interest. LDA measurement is noted before combustion, when the combustion process is started, LDA measurements should be recorded at specific time intervals, for example, 10 seconds.
- The autotransformer is used to run the fan at low speeds, this allows the user to obtain low ventilation values, below 0.70 m/s.

C. Safety Instructions

The following safety instructions should be followed by the researcher:

- Fuel bottles should be stored in a safe place away from any fire source.
- The researcher should wear an air filter face mask while conducting the LDA experiments, because long and repeated exposure to the tracing particles may affect the respiratory system.
- The researcher should wear laser safety glasses while the LDA system is on.
- The fuel should not be burned outside the combustion zone at any circumstances.
- All experiments should be conducted at ventilation velocities above 0.25 m/s, otherwise the transparent section's temperature will increase to high values that may fracture the glass.
- Gas lighters, which has a long probe, should be used to ignite the fuel to avoid any burns to the hand of the user.